



Synthesis of new *bis*(dimethylamino)benzophenone hydrazone for diabetic management: *In-vitro* and *in-silico* approach

Momin Khan^{a,*}, Ghulam Ahad^a, Aftab Alam^b, Saeed Ullah^c, Ajmal Khan^{c,**}, Kanwal^d, Uzma Salar^d, Abdul Wadood^e, Amar Ajmal^e, Khalid Mohammed Khan^{d,f}, Shahnaz Perveen^g, Jalal Uddin^h, Ahmed Al-Harrasi^{c,***}

^a Department of Chemistry, Abdul Wali Khan University, Mardan, 23200, Pakistan

^b Department of Chemistry, University of Malakand, Chakdara, Lower Dir, 18800, Pakistan

^c Natural & Medical Sciences Research Center, University of Nizwa, P.O Box 33, Postal Code 616, Birkat Al Mauz, Nizwa, Oman

^d H. E. J. Research Institute of Chemistry, International Center for Chemical and Biological Sciences, University of Karachi, Karachi, 75270, Pakistan

^e Department of Biochemistry, Abdul Wali Khan University, Mardan, 23200, Pakistan

^f Department of Clinical Pharmacy, Institute for Research and Medical Consultations (IRMC), Imam Abdulrahman Bin Faisal University, P.O. Box 31441, Dammam, Saudi Arabia

^g PCSIR Laboratories Complex, Karachi, Shahrah-e-Dr. Salimuzzaman Siddiqui, Karachi, 75280, Pakistan

^h Department of Pharmaceutical Chemistry, College of Pharmacy, King Khalid University, Abha, 62529, Kingdom of Saudi Arabia

ARTICLE INFO

Keywords:

4,4-Bis(dimethylamino)benzophenone
Schiff bases
 α -glucosidase inhibitors
Structure-activity relationship
Molecular docking

ABSTRACT

Inhibiting α -glucosidase is a reliable method for reducing blood sugar levels in diabetic individuals. *Bis*(dimethylamino)benzophenone derivatives **1–27** were synthesized from *bis*(dimethylamino)benzophenone via two-step reaction. Different spectroscopic techniques, including EIMS and ¹H NMR, were employed to characterize all synthetic derivatives. The elemental composition of synthetic compounds was confirmed by elemental analysis and results were found in agreement with the calculated values. The synthetic compounds **1–27** were evaluated for α -glucosidase inhibitory activity, except five compounds all derivatives showed good to moderate inhibitory potential in the range of $IC_{50} = 0.28 \pm 2.65 - 0.94 \pm 2.20 \mu M$. Among them, the most active compounds were **5**, **8**, **9**, and **12** with IC_{50} values of 0.29 ± 4.63 , 0.29 ± 0.93 , 0.28 ± 3.65 , and 0.28 ± 2.65 , respectively. Furthermore, all these compounds were found to be non-toxic on human fibroblast cell lines (BJ cell lines). Kinetics study of compounds **8** and **9** revealed competitive type of inhibition with K_i values 2.79 ± 0.011 and $3.64 \pm 0.012 \mu M$, respectively. The binding interactions of synthetic compounds were also confirmed through molecular docking studies that indicated that compounds fit well in the active site of enzyme. Furthermore, a total of 30ns MD simulation was carried out for the most potent complexes of the series. The molecular dynamics study revealed that compound-8 and compound-12 were stable during the MD simulation.

* Corresponding author.

** Corresponding author.

*** Corresponding author.

E-mail addresses: mominkhan@awkum.edu.pk (M. Khan), ajmalkhan@unizwa.edu.om (A. Khan), aharrasi@unizwa.edu.om (A. Al-Harrasi).

<https://doi.org/10.1016/j.heliyon.2023.e23323>

Received 1 June 2023; Received in revised form 30 November 2023; Accepted 30 November 2023

Available online 4 December 2023

2405-8440/© 2023 Published by Elsevier Ltd.

This is an open access article under the CC BY-NC-ND license

(<http://creativecommons.org/licenses/by-nc-nd/4.0/>).

1. Introduction

The enzyme α -Glucosidase (EC 3.2.1.20) is situated on the brush border surface of small intestinal cells. Its function involves the hydrolysis of the 1,4-glycosidic bond within starch, leading to the production of α -D-glucose [1]. The α -D-glucose produced during absorption enters the bloodstream, contributing to elevated postprandial hyperglycemia [2]. Inhibitors targeting this enzyme play a crucial role in the management of type II diabetes mellitus. Regulating the digestion and absorption of glucose can be instrumental in preventing diabetes and associated disorders [3–5]. Acarbose, miglitol, and voglibose are currently employed as clinically prescribed medications for managing type II diabetes mellitus [6]. These medications, namely acarbose, miglitol, and voglibose, function as α -glucosidase inhibitors. Unfortunately, they are accompanied by various side effects like diarrhea, abdominal discomfort, and flatulence. Consequently, their efficacy is deemed to be approximately 50 % lower compared to other anti-diabetic agents such as sulfonylurea and metformin. To enhance their effectiveness, these drugs are frequently administered in combination with other anti-diabetic agents [7–11]. Hence, synthetic chemists are exploring enzyme inhibitors associated with various diseases to develop options that are both safer and more efficient against specific targets [12]. Numerous synthetic compounds have been documented for diverse targets such as α -glucosidase, amylase, and cholinesterase. Additionally, there are existing reports on flavone-based hydrazone as inhibitors of α -glucosidase [13–15] (see Scheme 1).

Benzophenone, an organic compound, plays a crucial role in photochemical reactions. It serves as a reagent in organic chemistry and finds applications as a flavor ingredient, flavor enhancer, and perfume fixative in the perfumery industry. Additionally, it is employed as an additive in the formulation of plastics, coatings, and adhesives. Furthermore, it is utilized in the textile industry to protect materials from degradation caused by ultraviolet radiation [16]. Benzophenones has been used broadly as photophysical probes to recognize and map peptide-protein interaction [17]. A set of benzophenone derivatives was found to be excellent antimalarial agents against *Plasmodium berghei* in mice [18]. Benzophenone derivatives has been reported to possess a wide range of bio-activities such as antimicrobial, antifungal, anti-carcinogenic, anti-HIV [19], antioxidant [20], anticancer [21], anesthetic [22], anti-inflammatory [23], and urease inhibitory [24] activities. In literature, benzophenone-O-glycosides are reported as α -glucosidase inhibitors [25,26] (Figure-1).

In literature, a number of novel derivatives based on benzophenone moiety and other *bis*-Schiff have been documented to possess a range of biological activities. Arshia et al., had been synthesized benzophenone based semicarbazone, thiosemicarbazone and sulfonamide derivatives and tested them for their *in vitro* anti-glycemic and urease inhibitory potential with promising results [27–29]. Similar to this, Alam et al. reported the synthesis and α -glucosidase inhibitory activity of 4-nitroacetophenone based *bis*-Schiff base derivatives as excellent glucosidase inhibitors [30]. Keeping in mind the activities of *bis*-Schiff bases and various benzophenone derivatives we encouraged to synthesized novel benzophenone based *bis*-Schiff bases as promising α -glucosidase inhibitors [31] (Figure-1). Now, we intend to further evaluate this class for their anti-diabetic potential in order to get the more potent lead candidates. Herein, we describe the synthesis of *bis*-Schiff bases, its structural elucidation, α -glucosidase (*in vitro*) inhibitory activity, and *in silico* analysis.

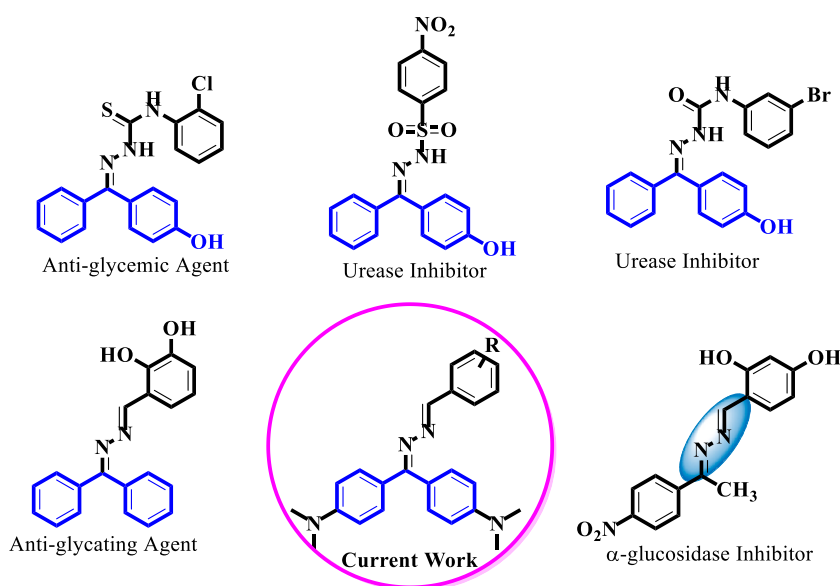


Figure-1. Rationale of the current study.

2. Result and discussions

2.1. Chemistry

Schiff bases 1–27 of 4,4'-(hydrazonomethylene)bis(N,N-dimethylaniline) were synthesized through a two-step reaction. The initial step involved the treatment of 4,4'-(hydrazonomethylene)bis(N,N-dimethylaniline) (commercially available) with hydrazine hydrate in excess, resulting in the hydrazone derivative [32]. In the second step, hydrazone derivative (I) underwent a reaction with various aromatic aldehydes having 4–5 drops glacial acetic acid, leading to the formation of a diverse array of Schiff bases 1–27 (Scheme-1, Table-1). In all cases, solid products were generated, filtered, washed with absolute ethanol, and subsequently dried under vacuum, yielding pure products in the form of fluffy solids. The structures of compounds 1–27 were elucidated through various spectroscopic techniques, including ^1H NMR, EI-MS and Elemental analysis.

2.2. α -Glucosidase inhibitory activity

The *in vitro* α -glucosidase inhibition studies were conducted for all synthesized Schiff bases (1–27) derived from the hydrazone of 4,4-bis(dimethylamino)benzophenone. Except compounds 11, 20, 21, 25 and 27, all the derivatives exhibited moderate to significant inhibitory potential in the range of $\text{IC}_{50} = 0.28 \pm 2.65 - 0.94 \pm 2.20 \mu\text{M}$ as compared to standard acarbose $\text{IC}_{50} = 0.27 \pm 2.43 \mu\text{M}$ (Table-2).

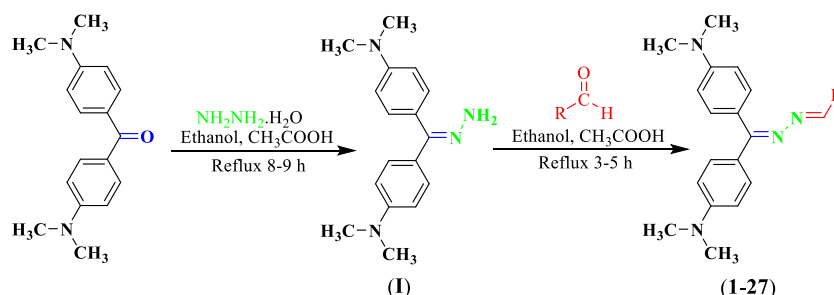
2.3. Structure-activity relationship (SAR)

Structure-activity relationship of the synthetic derivatives 1–27 was established on the basis of different substituents on aryl part. To understand the better structure-activity relationship the synthetic molecule is divided into two parts as shown in Figure-2.

Compounds 12 ($\text{IC}_{50} = 0.28 \pm 3.13 \mu\text{M}$) and 8 ($\text{IC}_{50} = 0.28 \pm 2.65 \mu\text{M}$) were found as the most potent compounds of the series and displayed comparable activity with the standard acarbose ($\text{IC}_{50} = 0.27 \pm 0.43 \mu\text{M}$). Compound 12 possess nitro group at *para* position while compound 8 have hydroxy and nitro groups at *ortho* and *meta* positions, respectively, The activity of both these compounds may stem from the presence of an electron-withdrawing nitro group, which could potentially interact effectively with the enzyme's active site (Figure-3).

Among hydroxy substituted compounds, compound 4 ($\text{IC}_{50} = 0.33 \pm 2.64 \mu\text{M}$) bearing two hydroxy groups at *ortho* and *meta* positions showed good inhibitory potential. Changing the position of one of the hydroxy group from *ortho* to *para* resulted in slight decreased activity as in compound 17 ($\text{IC}_{50} = 0.35 \pm 1.26 \mu\text{M}$), however, shifting the position of one of the hydroxy from *meta* to *para* resulted in two folds declined activity in compound 2 ($\text{IC}_{50} = 0.68 \pm 0.29 \mu\text{M}$) which showed that substituent at *meta* position is contributing in the activity. Compound 1 ($\text{IC}_{50} = 0.39 \pm 0.88 \mu\text{M}$) having one hydroxy group at *meta* position of aryl part was also found to be active but was slightly less active as compared to its di hydroxy analogue 4, however shifting the position of hydroxy from *meta* to *ortho* and *para* in compounds 7 ($\text{IC}_{50} = 0.58 \pm 2.24 \mu\text{M}$) and 26 ($\text{IC}_{50} = 0.82 \pm 1.12 \mu\text{M}$), respectively, showed decreased activity as compared to compound 1. The activity of these monohydroxy substituted compounds is less than the dihydroxy compounds which means that both hydroxy groups are actively participating in enzyme inhibition, it was also observed that *meta* substituted compound was more active as compared to *ortho* and *para* substituted compounds. Compound 20 with tri hydroxy groups was completely inactive which showed that addition of another hydroxy resulted in complete loss of activity (Figure-4).

Compound 5 ($\text{IC}_{50} = 0.29 \pm 4.67 \mu\text{M}$) having bromo group at *ortho* position was most active amongst the halogen substituted derivatives and showed comparable activity with the standard acarbose ($\text{IC}_{50} = 0.27 \pm 0.43 \mu\text{M}$). However, compound 13 ($\text{IC}_{50} = 0.72 \pm 1.44 \mu\text{M}$) bearing chloro group at *ortho* position was less active as compared to compound 5. Shifting the position of chloro group from *ortho* to *para* resulted in increased inhibitory activity in compound 18 ($\text{IC}_{50} = 0.31 \pm 1.12 \mu\text{M}$) might be due to the better interaction of chloro group with the active site of enzyme. The dichloro substituted compound 3 ($\text{IC}_{50} = 0.77 \pm 0.64 \mu\text{M}$) having two chloro groups at *ortho* and *para* positions was less active as compared to compounds 18 and 13. It showed that bromo group is enhancing the activity, however, replacing the bromo group from chloro resulted in decreased activity and the position of substituents also played an important role in activity. Nevertheless, compound 21 with mixed substitution of hydroxy and bromo was found to be



Scheme-1. Synthetic Procedure of Schiff bases derived from the hydrazone of 4,4-bis(dimethylamino)benzophenone 1–27.

Table-1
Different Schiff base derivatives 1–27 of 4,4-bis(dimethylamino)benzophenone hydrazone.

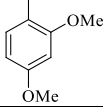
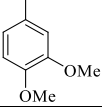
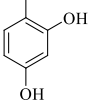
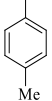
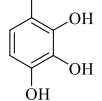
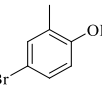
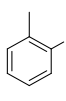
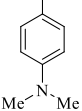
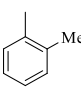
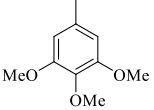
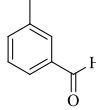
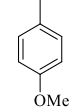
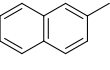
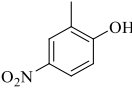
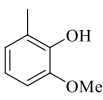
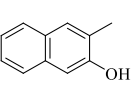
C. No	R	C. No	R	C. No	R
1		10		19	
2		11		20	
3		12		21	
4		13		22	
5		14		23	
6		15		24	
7		16		25	
8		17		26	
9		18		27	

Table-2
Docking scores (S) and α -glucosidase inhibitory potential of compounds 1–27.

Comp. No.	Docking Score (S)	IC ₅₀ ± SEM ^a (μM)	Comp. No.	Docking Score (S)	IC ₅₀ ± SEM ^a (μM)
1	-12.856126	0.39 ± 0.88	15	-11.919278	0.49 ± 1.43
2	-11.496664	0.68 ± 0.29	16	-11.523767	0.43 ± 2.39
3	-11.232298	0.77 ± 0.64	17	-12.294073	0.35 ± 1.26
4	-13.705235	0.33 ± 2.64	18	-13.710643	0.31 ± 2.93
5	-13.964074	0.29 ± 4.67	19	-12.849945	0.31 ± 1.59
6	-12.62954	0.36 ± 2.69	20	-7.007668	NA ^b
7	-12.01612	0.58 ± 2.24	21	-7.765608	NA ^b
8	-13.947351	0.28 ± 2.65	22	-11.9946	0.45 ± 0.91
9	-12.91043	0.29 ± 0.93	23	-12.566521	0.35 ± 0.91
10	-12.62954	0.38 ± 2.27	24	-10.181315	0.94 ± 2.21
11	-6.466705	NA ^b	25	-7.778631	NA ^b
12	-13.934394	0.28 ± 3.13	26	-11.649983	0.82 ± 1.12
13	-11.740894	0.72 ± 1.44	27	-8.831872	NA ^b
14	-12.562585	0.51 ± 1.84	Acarbose ^c	-13.183158	0.27 ± 0.43

SEM^a (Standard error mean); NA^b (Not active); Acarbose^c (Standard inhibitor for α -glucosidase inhibitory activity).

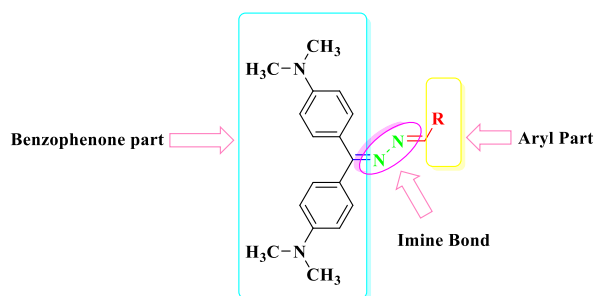


Figure-2. Common structure of bis-Schiff base 1–27.

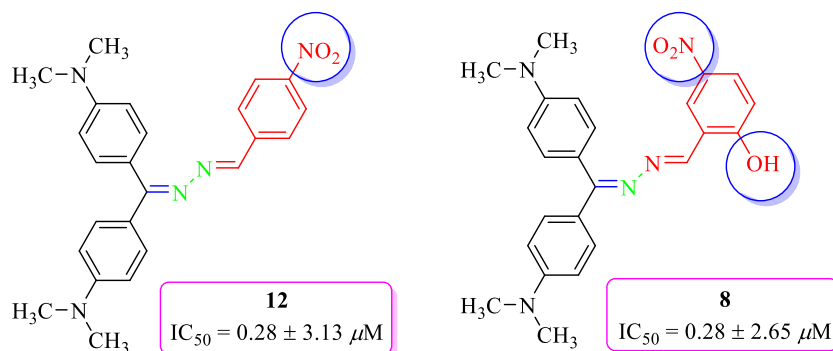


Figure-3. Structure-activity relationship of compounds 12 and 8.

inactive (Figure-5).

Among methoxy substituted derivatives, compound 24 ($IC_{50} = 0.94 \pm 2.21 \mu M$) bearing methoxy group at *para* position was found to be active. Addition of another methoxy at *ortho* position of aryl part resulted in increased activity in compound 10 ($IC_{50} = 0.38 \pm 2.27 \mu M$) might be due to better interaction of *ortho* substituted methoxy group. Shifting the position of one of methoxy groups from *ortho* to *meta* lead to further enhanced activity in compound 19 ($IC_{50} = 0.31 \pm 1.59 \mu M$). Compound 6 ($IC_{50} = 0.36 \pm 2.69 \mu M$) having three methoxy groups at *meta* and *para* positions exhibited a slight decrease in activity as compared to compound 19. Compound 9 ($IC_{50} = 0.29 \pm 0.93 \mu M$) having hydroxy and methoxy at *ortho* and *meta* positions was also found to have good inhibitory potential and showed comparable activity with the standard acarbose ($IC_{50} = 0.27 \pm 0.43 \mu M$) (Figure-6).

The methyl substituted derivative 23 ($IC_{50} = 0.35 \pm 0.91 \mu M$) having methyl group at *ortho* position also exhibited good inhibitory activity. However, shifting the position of methyl group from *ortho* to *para* in compound 11 resulted in complete inactivity. Compound 22 ($IC_{50} = 0.45 \pm 0.91 \mu M$) bearing thiomethyl group at *para* position of aryl part was also found to be active but it was less active as compared to the standard. Compound 14 ($IC_{50} = 0.51 \pm 1.84 \mu M$) having *N,N*-dimethyl aniline part at *para* position was also found to have weak inhibitory activity. Compound 15 ($IC_{50} = 0.49 \pm 1.43 \mu M$) bearing an aldehyde group at *para* position showed good inhibitory activity. Compound 16 ($IC_{50} = 0.43 \pm 2.39 \mu M$) with naphthyl ring exhibited good activity, however, addition of hydroxy at this naphthyl ring resulted in complete inactivity in compound 27 (Figure-7).

The above pattern showed that methoxy, nitro, and hydroxy groups are mainly participating in the inhibitory activity of enzyme. It was also observed that the particular positions of different groups are also contributing to the activity. All derivatives (1–27) were evaluated for their cytotoxicity against normal BJ (human fibroblast) cell lines in which all the derivatives showed inactivity at $30 \mu M$. These promising findings, insight the therapeutic potential of these new investigated inhibitors in the management of diabetes. Because the α -glucosidase in the key metabolic enzyme of carbohydrates and its inhibition is a promising target to overcome on the elevated level of glucose. Therefore, these inhibitors have high potential to be used as anti-diabetic drug candidate molecules.

2.4. Kinetic studies

The most potent compounds 8 and 9 were selected to reveal their mechanism of action. Compounds 8 and 9 displayed concentration dependent pattern of inhibition with K_i values 2.79 ± 0.0011 and $3.64 \pm 0.0012 \mu M$. In such type of inhibition inhibitors bind with the active site residues of the α -glucosidase therefore, K_m value increases while V_{max} of the enzyme remains constant (Fig. 8). (Fig. 8A and D). The K_i values were calculated by plotting the slope of each line in the Lineweaver-Burk plots against different concentrations of compounds 8 and 9 (Fig. 8B and E). The K_i value was established from Dixon plot by plotting the reciprocal of the rate of reaction beside diverse concentrations of compounds 8 and 9 (Fig. 8C and F). As the worth of competitive inhibitors is more because most of the drugs available are competitive inhibitors and they are concentration dependent. In these contexts, both compounds 8 and

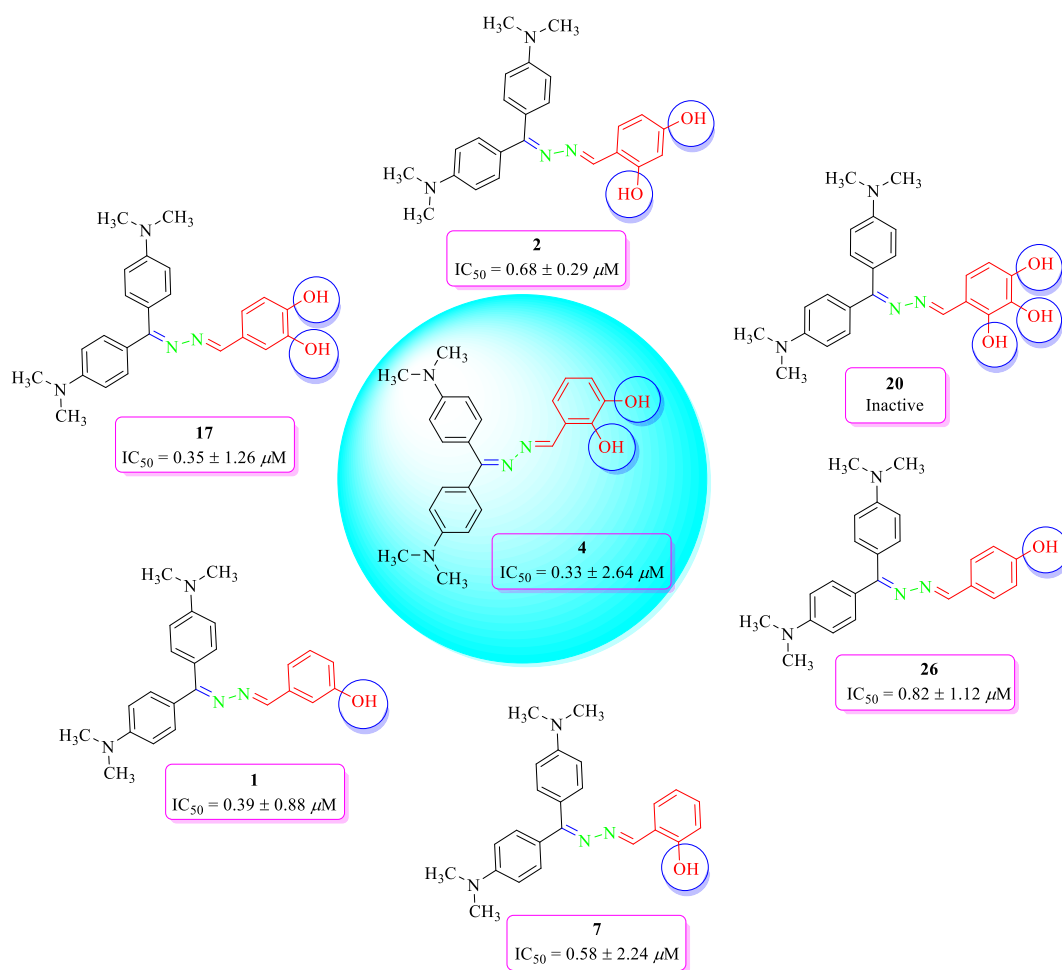


Figure-4. Structure-activity relationship of compounds 1, 2, 4, 7, 17, 20, and 26.

9 are identified as competitive type of inhibitors. Due to its mode of inhibition these inhibitors validate a crucial step in the drug candidates' small molecules.

2.5. In-silico study

The top ranked conformations of each docked ligand were saved for further evaluation in a separate database. The docking scores well correlated with the experimental results as shown in [Table-2](#). For example, the most active compounds 5, 8, 9, and 12 were ranked as top scorer compounds whereas the least active/non-active compounds were ranked with lower/poor docking scores ([Table-2](#)).

2.6. Interactions detail of ligands and protein

According to the IC_{50} values, the top four compounds 5, 8, 9, and 12 were found to show significant interactions with target protein along with good docking scores. Compound 5 is one of the most active compounds shown in [Figure-9A](#) was bound deeply into the binding cavity of α -glucosidase forming five interactions with the residues His348, Asp408, Phe311, Arg312, and Phe157. His348 is involved in π -hydrogen interaction with the $N(CH_3)_2$ group of N,N -dimethylaniline. Asp408 formed a polar contact with the bromophenyl moiety whereas Phe311 and Arg312 both formed π -hydrogen interactions with the same bromo-phenyl group. Phe157 showed a π - π interaction with the π -electrons of the second N,N -dimethylaniline moiety of the compound.

Compound 8, another most active compound also formed five prominent interactions with the binding site residues Arg312, Asp214, His245, and Phe157 as shown in [Figure-9B](#). Arg312 showed a hydrogen bonding interaction with the nitro (NO_2) group of the compound. An induced polar hydrogen donor interaction was observed between Asp214 and the nitro-phenol group. Two π -hydrogen interactions were observed between His245 and N,N -dimethylaniline moiety. Likewise compound 5, Phe157 showed a π - π interaction with the π -electrons of the N,N -dimethylaniline moiety of the compound.

Compound 9 can be seen clearly in [Figure-9C](#) forming four interactions contacts with the residues His245, Asp214, Tyr71, and

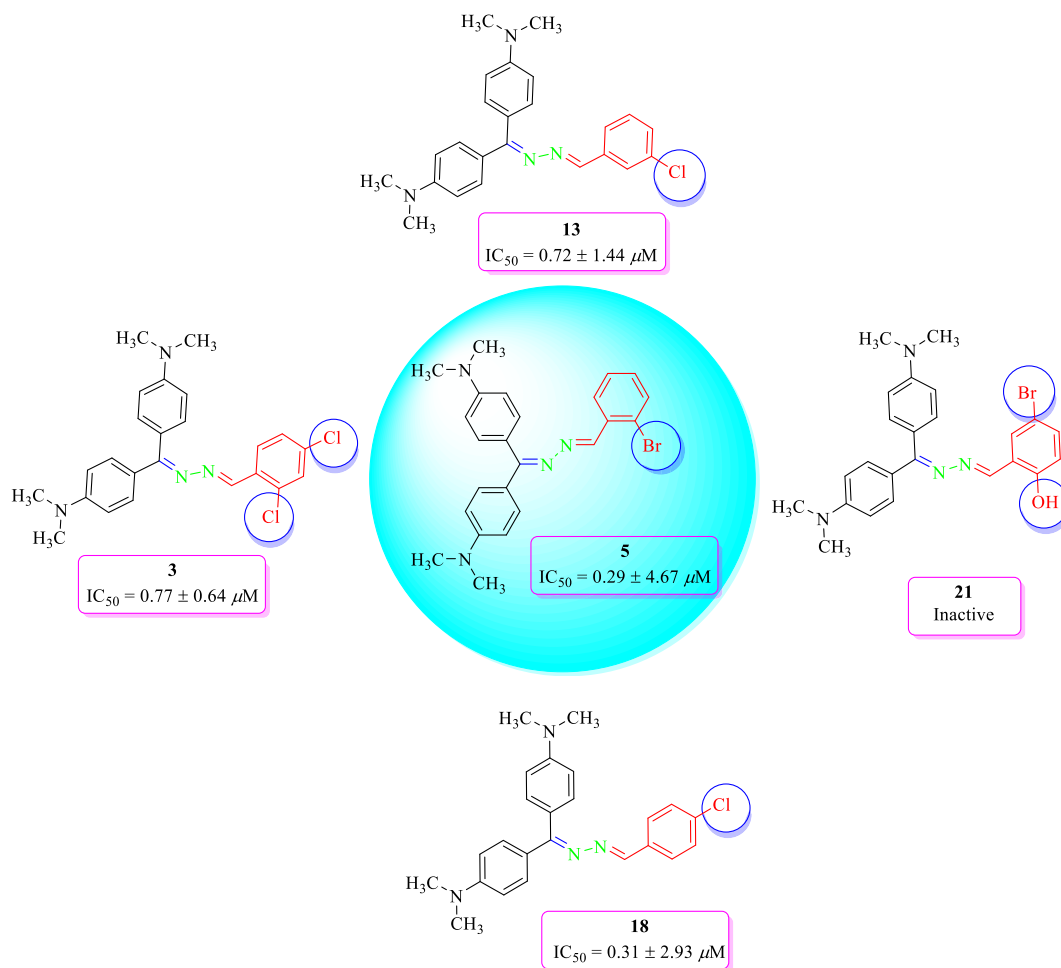


Figure-5. Structure-activity relationship of compounds 3, 5, 13, 18, and 21.

Phe1577. His245 was involved in a π -hydrogen interaction with the *N,N*-dimethylaniline group. Like compound 8, an induced polar hydrogen donor interaction was also observed here between Asp214 and the nitro-phenol group. Tyr71 was also found within a distance of π -hydrogen contact with the same nitro-phenol moiety. Phe157 showed a π - π interaction with the π -electrons of the *N,N*-dimethylaniline moiety of the compound just like the above-mentioned compounds.

Another significantly active compound 12 in this group showed three different interactions with the residues His245, His248, and Phe157 as shown in **Figure-9D**. His245 participated in a π -hydrogen interaction with the *N,N*-dimethylaniline group, while His348 was observed engaging in a hydrogen interaction with the nitro-phenol group. Phe157 here also showed a π - π interaction with the π -electrons of the *N,N*-dimethylaniline moiety of the compound just like all the above-mentioned compounds.

The structural feature observed in this group for good interaction mode and active nature of compound is the presence of an electron withdrawing group like halogen and nitro (NO_2) groups, *N,N*-dimethylaniline, and the π electron system of all phenyl groups. As a whole, all the active compounds showed good *in silico* inhibition of the target enzyme as reflected from the corresponding docking scores calculated for each compound. The correlation coefficient calculated ($R^2 = 0.732$) for predicted docking score and IC_{50} values of active compounds indicates good agreement between the docking and experimental results. The correlation graph is shown in **Figure-10**.

Furthermore, Lipinski's rule of five, also known as the Pfizer rule of five, is widely used for the evaluation of drug-likeness of compounds. Lipinski's rule of five states that drug-like compounds have molecular weight <500 Da, $\log P < 5$, H-bond donor <5, and H-bond acceptor <10. All the tested compounds were filtered out using the Lipinski rule of 5. Most of the compounds obeyed these rules. **Table 3** shows the drug-likeness of the tested compounds calculated by MOE software.

2.7. MD simulation analysis

2.7.1. Root mean square deviation analysis (RMSD)

The stability of the system is inversely associated with the amplitudes of the fluctuations. A higher RMSD value indicated higher

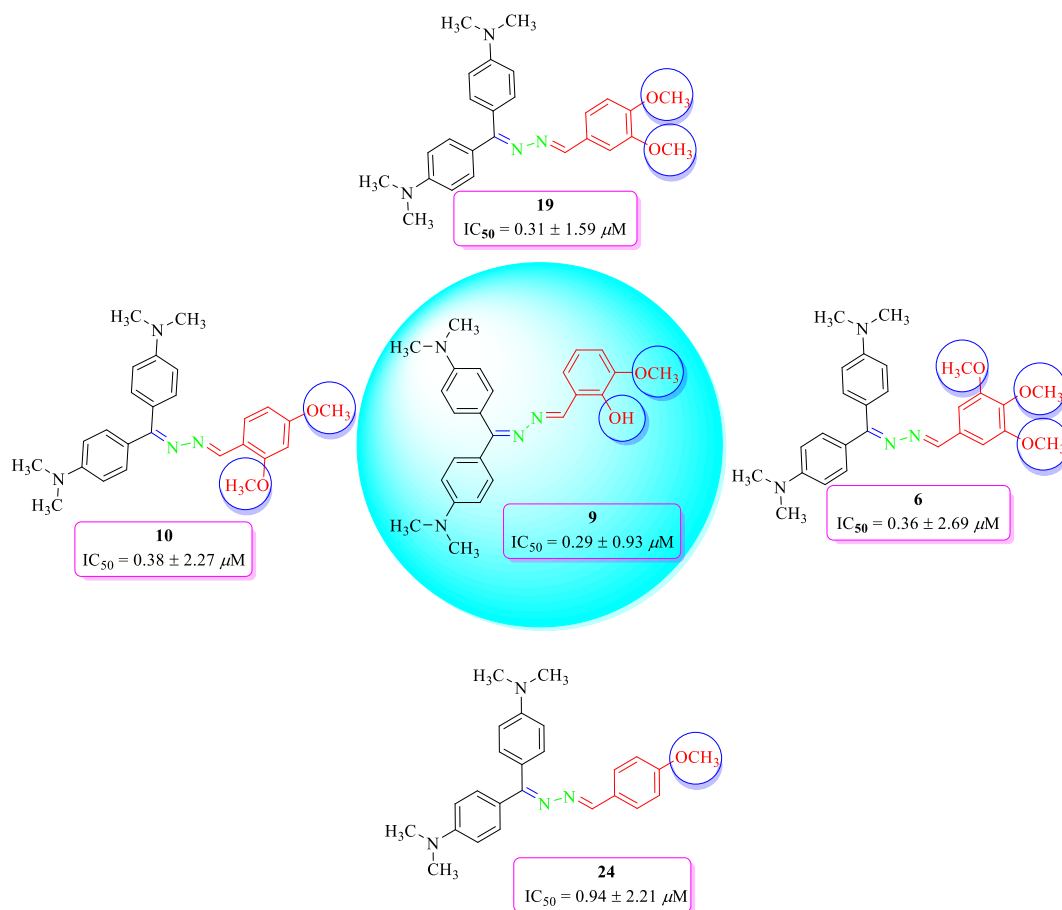


Figure-6. Structure-activity relationship of compounds 6, 9, 10, 19, and 24.

fluctuations and a decrease in the stability of the systems. The average RMSD of the system α -glucosidase\compound 12 was found to be 2.9 Å. Some major fluctuations were observed during 5–15ns after that the system gain stability and remained stable till 30ns MD simulation. The average RMSD value of α -glucosidase\compound 8 and α -glucosidase\acarbose were found to be 1.9 and 1.7 Å respectively. The complex α -glucosidase \compound 8 remained highly stable throughout the MD simulation except for some minor deviations during 18–25ns. On the other hand, the complex α -glucosidase\acarbose showed high stability during the entire 30ns MD simulation however, some minor fluctuations during 12–18ns and 22–25ns were observed. Fig. 11 shows the RMSD plots for all the complexes. A previous study reported that out of the total amino acids in α -glucosidase, 35 % are helices, 25 % are β sheets, and 38 % are coil regions [33]. During MD simulation fluctuations were mainly observed in the loop regions while all other regions of the protein were found to be stable.

2.7.2. Root mean square fluctuation analysis (RMSF)

To evaluate the dynamic behavior of protein residues when bound to the ligands, root-mean-square fluctuations (RMSF) values were computed. RMSF analysis revealed that residues other than the active site region showed higher fluctuations. The active site residues including Phe157, Asp214, His245, Phe311, Arg312, Asp408, and His348 showed less fluctuations and revealed stable behavior throughout the MD simulation. RMSF analysis indicates that the binding site residues made strong interactions with the ligands. Fig. 12 displays the RMSF plots for all the complexes.

2.7.3. Radius of gyration analysis (Rg)

To identify the compactness of protein and ligand complexes the radius of gyration (Rg) of the carbon alpha atoms was calculated. The Rg value for α -glucosidase\compound12, α -glucosidase \compound8 and α -glucosidase\acarbose were found to be 19.4–20.0, 19.3–19.6, and 19.0–19.5 Å respectively. Overall, the α -glucosidase\compound8 and α -glucosidase\acarbose protein-ligand complexes showed that there were no unfolding events or loose packing and emphasized the highly compact structure of the complexes whereas the α -glucosidase\compound12 revealed slightly unstable behavior during the MD simulation. Fig. 13 shows the RoG plots for all the complexes.

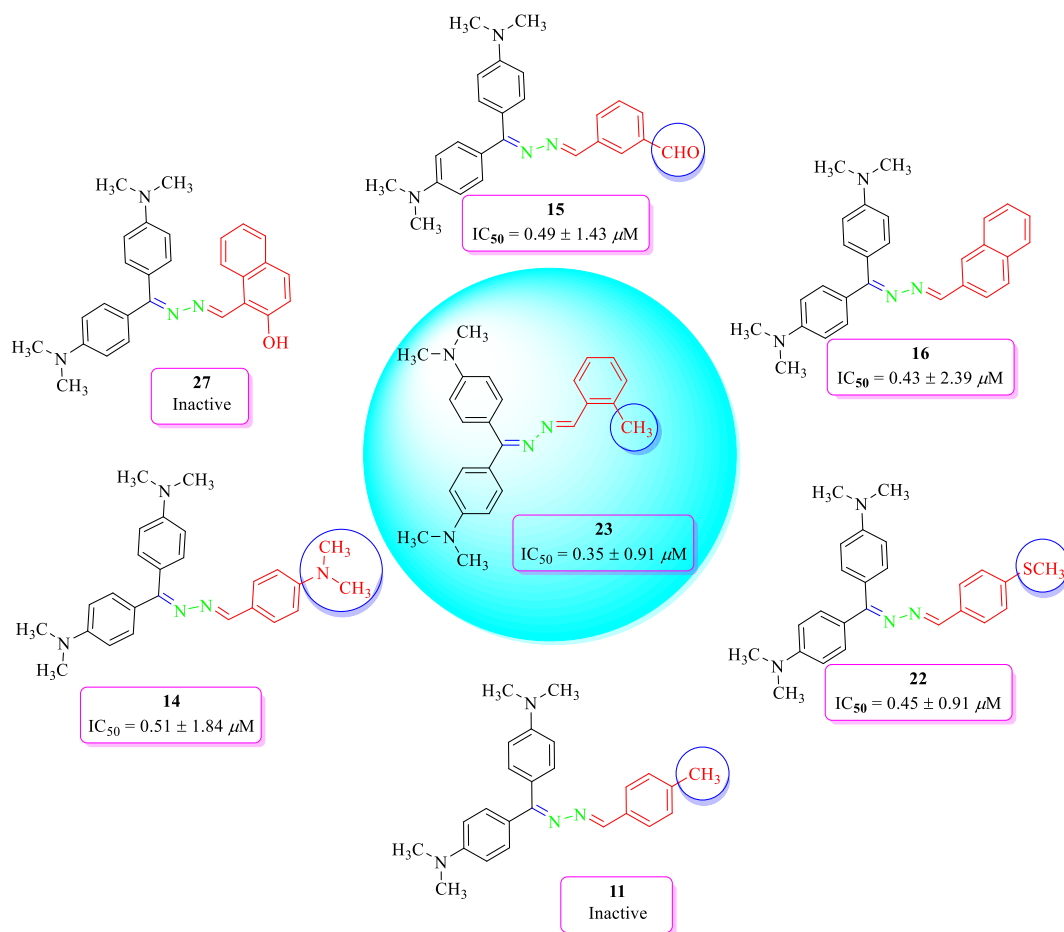


Figure-7. Structure-activity relationship of compounds 11, 14, 15, 16, 23, and 27.

3. Experimental

3.1. Materials and methods

The molar masses of compounds were confirmed by Finnigan MAT-311 equipment (Germany) and obtain its electron impact mass spectra (EI-MS). The 1H NMR spectra in $DMSO-d_6$ were carried out on Bruker AVANCE 400 MHz spectrophotometer. Coupling constant are expressed in Hz, and chemical shift are reported in δ (ppm), similar to this, s (singlet), d (doublet), t (triplet), q (quartet), and m (multiplet) were used as splitting pattern. Thin layer chromatography on Kieselgel 60, 254 pre-coated silica gel aluminum plates were used for the progression of all reactions and the spots were visualized by utilizing UV lamp at 254 nm. The synthesis and characterization of the titled compounds were conducted successfully.

3.2. Synthetic procedure of compounds 1-27

A mixture comprising 4,4-bis(dimethylamino)benzophenone (1 g) and hydrazine hydrate (10 mL) was refluxed for 8–9 h, yielding 4,4'-(hydrazonomethylene)bis(N,N-dimethylaniline) (I). The reaction progress was monitored via TLC analysis. The reaction mixture was then poured onto crushed ice, resulting in precipitates that were filtered and air-dried. In the second step, 4,4'-(hydrazonomethylene)bis(N,N-dimethylaniline) (I) (1 mmol) was treated with a number of different benzaldehydes (substituted) (1 mmol) in absolute ethanol (10 mL) with a little quantity of acetic acid, and the mixture was refluxed for 3–5 h. Completion of the reaction was confirmed by TLC analysis. After completion, the reaction mixture was cooled, leading to the formation of crystals that were collected and recrystallized from ethanol to obtain pure crystals. The structural elucidation of all these product derivatives (1–27) was confirmed utilizing EI-MS and 1H NMR spectroscopy.

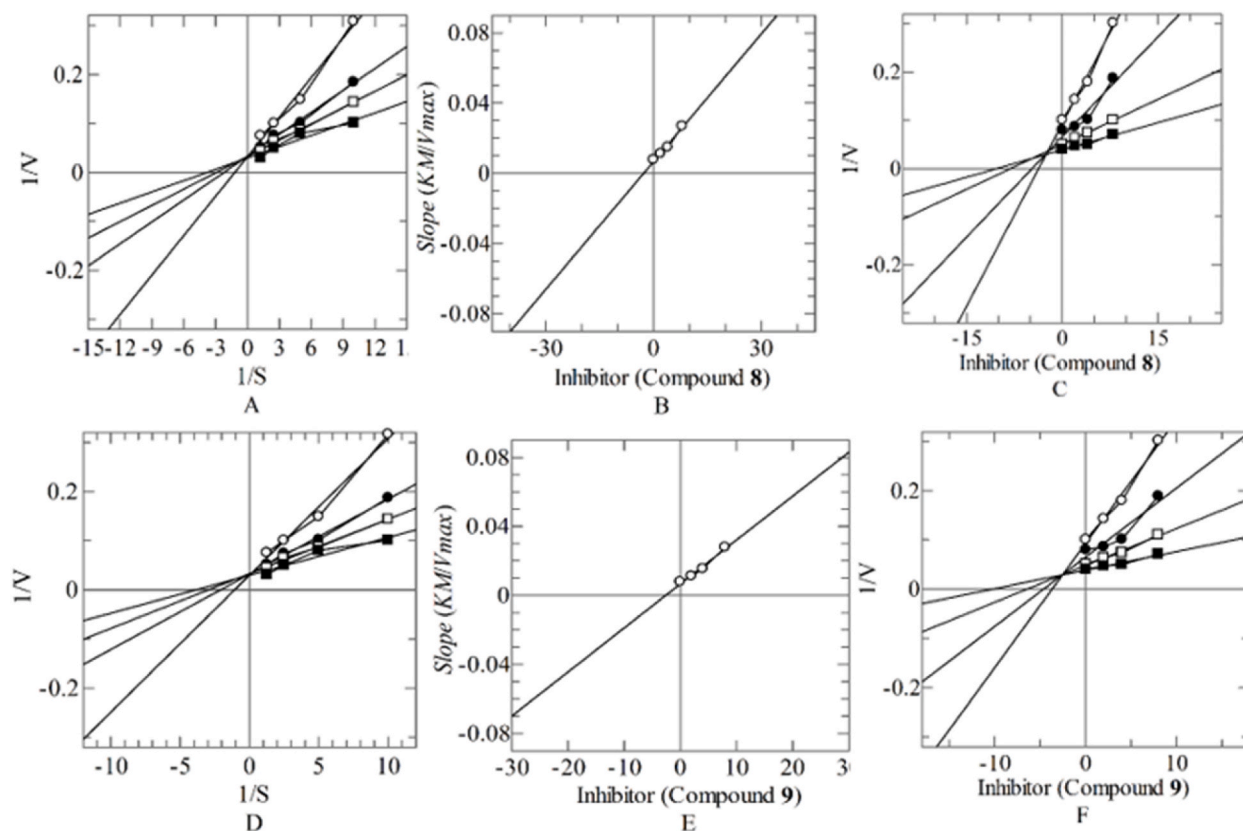


Figure-8. Mode of inhibition of α -glucosidase by compound 8, 9 (A, D) Line weaver-Burk plot of reciprocal of rate of reaction (velocities) vs reciprocal of substrate 4-nitro phenyl- α -D-glucopyranoside in the absence of (■), and in the presence of 8.00 μ M (○), 4.00 μ M (●), and 2.00 μ M (□) of compound 8, 9. (B, E) Secondary replot of Line weaver-Burk plot between the slopes of each line on-Line weaver-Burk plot vs different concentrations of compound 8, 9. (C, F) Dixon plot of reciprocal of rate of reaction (velocities) vs different concentrations of compound 8, 9.

3.3. 2-*[bis-(4-dimethylamino-phenyl)-methylene]-hydrazonomethyl*}-phenol (1)

Yield: 0.25 g (87 %); $^1\text{H NMR}$ (400 MHz, $\text{DMSO-}d_6$): δ 2.97 (s, 12H, $-\text{NCH}_3$), 6.15 (d, $J = 2.4$ Hz, 1H, H-2''), 6.33 (m, 2H, H-4''/5''), 6.70 (d, $J = 8.8$ Hz, 2H, H-3/5), 6.76 (d, $J = 8.8$ Hz, H-3'/5'), 7.08 (d, $J = 8.8$ Hz, 2H, H-2'/6'), 7.28 (d, $J = 8.4$ Hz, 1H, H-6''), 7.46 (d, $J = 8.8$ Hz, 2H, H-2/6), 8.69 (s, 1H, =CH), 11.68 (br.s, 1H, -OH); EI-MS m/z (% rel. abund.): 386 (M^+ , 100), 92 (15), 126 (35), 226 (20), 266 (83), 293 (13); Anal. calcd. for $\text{C}_{24}\text{H}_{26}\text{N}_4\text{O}$: (386.48): N, 14.50; H, 6.78; C, 74.58; Found: N, 14.51; H, 6.76; C, 74.57.

3.4. 4-*[bis-(4-dimethylamino-phenyl)-methylene]-hydrazonomethyl*}-benzene-1,3-diol (2)

Yield: 0.235 g (84 %); $^1\text{H NMR}$ (400 MHz, $\text{DMSO-}d_6$): δ 2.96 (s, 12H, $-\text{NCH}_3$), 6.34 (dd, 1H, H-5''), 6.75 (d, $J = 8.8$ Hz, 2H, H-3/5), 6.77 (d, $J = 8.8$ Hz, 2H, H-3'/5'), 7.09 (d, $J = 8.8$ Hz, 2H, H-2'/6'), 7.28 (d, $J = 8.4$ Hz, 1H, H-6''), 7.45 (d, $J = 8.8$ Hz, 2H, H-2/6), 8.68 (s, 1H, =CH), 11.67 (br.s, 2H, -OH); EI-MS m/z (% rel. abund.): 400 (M^+ , 100), 126 (22), 223 (22), 250 (13), 266 (68), 385 (21); Anal. calcd. for $\text{C}_{26}\text{H}_{28}\text{N}_2\text{O}_2$: (400.51): N, 6.99; H, 7.05; C, 77.97; Found: N, 6.97; H, 7.06; C, 77.96.

3.5. Bis-(4-dimethylamino-phenyl)-methylene-hydrazonomethyl-2,4-dichloro-benzene (3)

Yield: 0.23 g (88 %); $^1\text{H NMR}$ (400 MHz, $\text{DMSO-}d_6$): δ 2.96 (s, 12H, $-\text{NCH}_3$), 6.75 (d, $J = 8.8$ Hz, 4H, H-3/5, H-3'/5'), 7.12 (d, $J = 8.4$ Hz, 1H, H-3''), 7.49 (d, $J = 8.4$ Hz, 2H, H-5''/6''), 7.59 (d, $J = 8.8$ Hz, 2H, H-2'/6'), 7.79 (d, $J = 8.8$ Hz, 2H, H-2/6), 8.68 (s, 1H, =CH); EI-MS m/z (% rel. abund.): 439 (M^+ , 100), 148 (67), 224 (34), 251 (24), 268 (68), 380 (36); Anal. calcd. for $\text{C}_{24}\text{H}_{24}\text{Cl}_2\text{N}_4$: (439.38): N, 12.75; H, 5.51; C, 65.61; Found: N, 12.74; H, 5.50; C, 65.62.

3.6. 3-*[bis-(4-dimethylamino-phenyl)-methylene]-hydrazonomethyl*}-benzene-1,2-diol (4)

Yield: 0.263 g (83 %); $^1\text{H NMR}$ (400 MHz, $\text{DMSO-}d_6$): δ 2.96 (s, 12H, $-\text{NCH}_3$), 6.72 (d, $J = 8.4$ Hz, 4H, H-3/5, H-3'/5'), 6.81 (m, 2H, H-4''/5''), 6.95 (d, $J = 8.8$ Hz, 1H, H-6''), 7.12 (d, $J = 8.4$ Hz, 2H, H-2'/6'), 7.49 (d, $J = 8.8$ Hz, 2H, H-2/6), 8.68 (s, 1H, =CH), 11.67 (br.

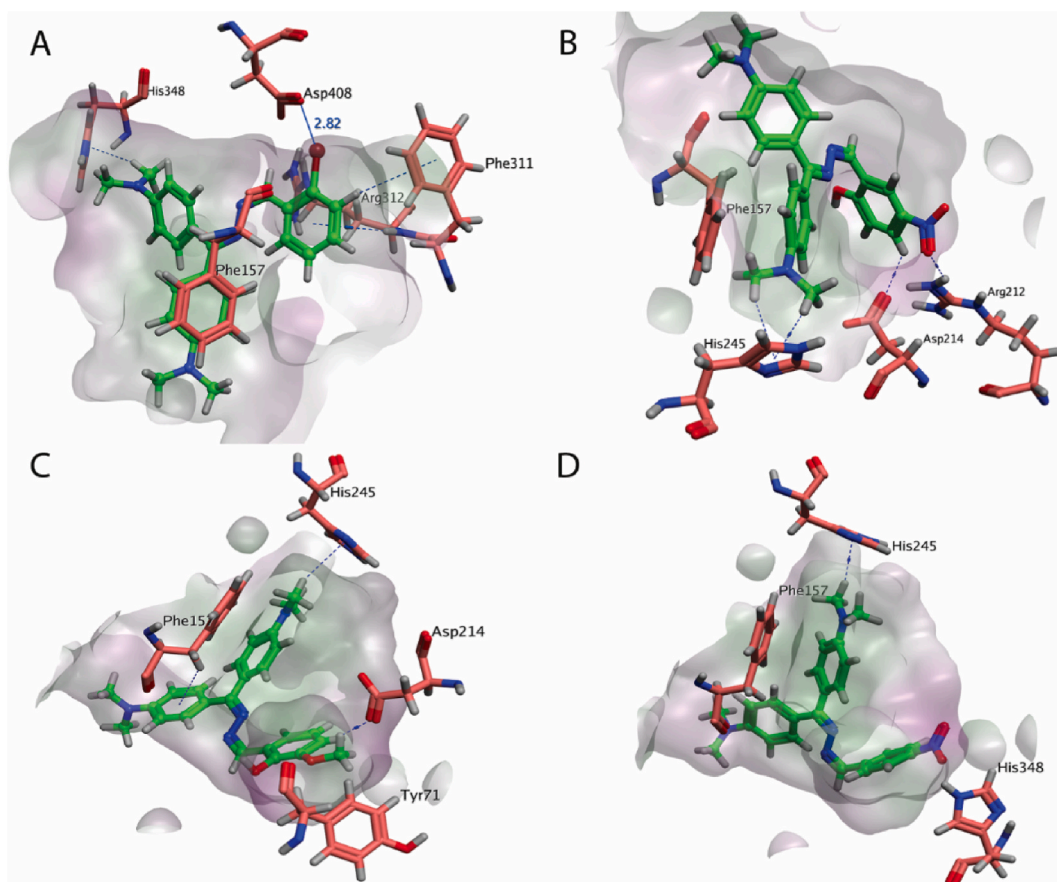


Figure-9. Three-dimensional interaction of compounds 5, 8, 9, and 12 with active site residues of α -glucosidase. Ligands are shown in light green color, key residues of the active site are shown in orange stick mode, and hydrogen bonding and other interaction is shown in dark color dotted lines. (A) Hydrogen bonding and polar interaction of compound 5 with the active site residues (B) 3D interactions network of compound 8 (C) 3D interactions network of compound 9 (D) 3D interaction of compound 12.

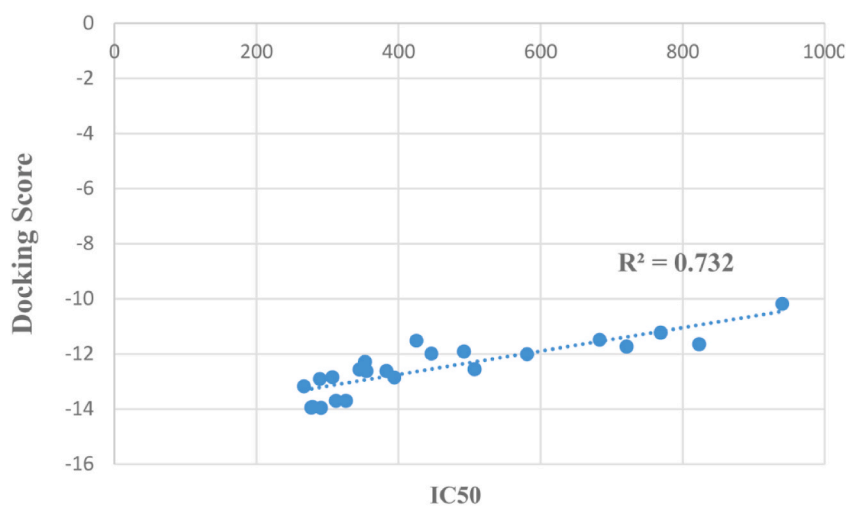


Figure-10. Correlation graph between predicted docking scores and calculated IC₅₀ values.

Table 3

Drug likeness of all the synthesized compounds.

S. No	Molecular Weight (g/mol)	H-bond donor	H-bond acceptor	logP
1	386.50	1	3	4.80
2	402.50	2	4	4.32
3	439.39	0	2	6.65
4	402.50	2	4	4.27
5	449.40	0	2	6.10
6	412.58	0	2	6.73
7	386.50	1	3	4.78
8	431.50	1	3	4.84
9	416.52	1	4	4.70
10	430.55	0	4	5.11
11	384.53	0	2	5.76
12	415.50	0	2	5.27
13	404.94	0	2	5.97
14	413.57	0	2	5.39
15	398.51	0	3	5.25
16	434.59	0	2	4.44
17	402.50	2	4	4.27
18	404.94	0	2	5.97
19	430.55	0	4	5.11
20	418.50	3	5	3.81
21	465.39	1	3	5.66
22	416.59	0	2	5.76
23	384.53	0	2	5.76
24	400.53	0	3	5.19
25	413.57	0	4	5.16
26	386.50	1	3	4.78
27	450.59	1	3	6.09

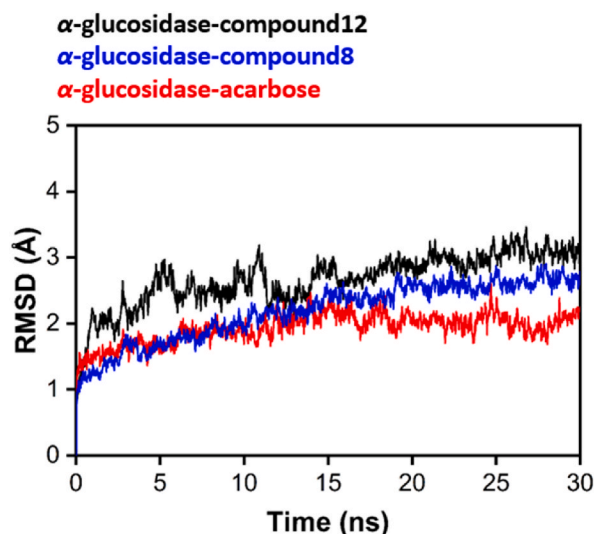


Fig. 11. RMSD plots of all the complexes α -glucosidase\compound 12 (Black) α -glucosidase\compound 8 (Blue) and α -glucosidase\acarbose (Red). The X-axis shows time in ns while the Y-axis shows the value of RMSD.

s, 2H, -OH); EI-MS m/z (% rel. abund.): 402 (M^+ , 100), 126 (17), 223 (23), 250 (14), 266 (80); Anal. calcd. for $C_{24}H_{26}N_4O_2$: (402.48): N, 13.92; H, 6.51; C, 71.62; Found: N, 13.93; H, 6.52; C, 71.61.

3.7. Bis-(4-dimethylamino-phenyl)-methylene-hydrazone-methyl-2-bromo-benzene (5)

Yield: 0.250 g (86 %); 1H NMR (400 MHz, $DMSO-d_6$): δ 2.96 (s, 12H, - NCH_3), 6.73 (d, $J = 8.8$ Hz, 4H, H-3/5, H-3'/5'), 7.12 (d, $J = 8.4$ Hz, 2H, H-2/6), 7.39 (m, 2H, H-4''/5''), 7.48 (d, $J = 8.8$ Hz, 2H, H-2'/6'), 7.69 (d, $J = 7.6$ Hz, 1H, H-3''), 7.77 (d, $J = 7.6$ Hz, 1H, H-6''), 8.68 (s, 1H, =CH); EI-MS m/z (% rel. abund.): 449 (M^+ , 100), 65 (13), 92 (24), 122 (29), 208 (16); Anal. calcd. for $C_{24}H_{25}BrN_4$: (449.38): N, 12.47; H, 5.61; C, 64.14; Found: N, 12.49; H, 5.60; C, 64.15.

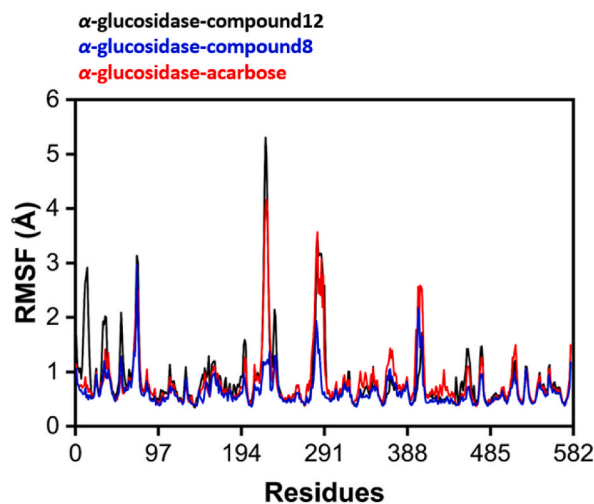


Fig. 12. RMSF plots of all the complexes α -glucosidase\compound 12 (Black) α -glucosidase\compound 8 (Blue) and α -glucosidase\acarbose (Red). The X-axis shows number of residues while the Y-axis shows the value of RMSF.

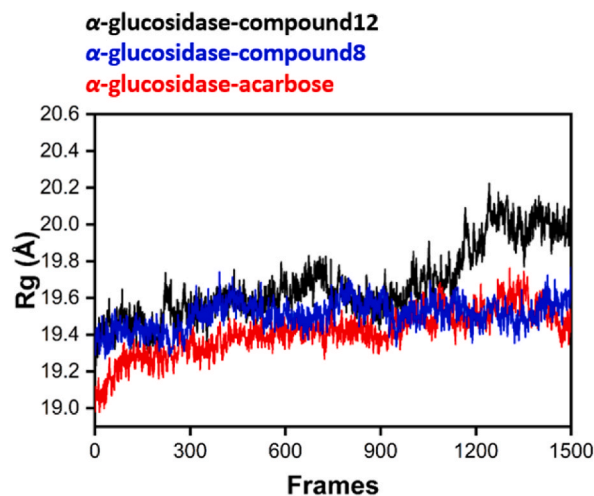


Fig. 13. Rg plots of all the complexes α -glucosidase\compound 12 (Black) α -glucosidase\compound 8 (Blue) and α -glucosidase\acarbose (Red). The X-axis shows number of frames while the Y-axis shows the value of Rg.

3.8. Bis-(4-dimethylamino-phenyl)-methylene-hydrazone-methyl-3,4,5-trimethoxy-benzene (6)

Yield: 0.241 g (83 %); $^1\text{H NMR}$ (400 MHz, $\text{DMSO-}d_6$): δ 2.96 (s, 12H, $-\text{NCH}_3$), 3.75 (s, 9H, $-\text{OCH}_3$), 6.73 (d, $J = 8.8$ Hz, 2H, H-3'/5'), 6.76 (d, $J = 8.8$ Hz, 2H, H-3/5), 7.02 (bd.s, 1H, H-2''), 7.16 (d, $J = 8.8$ Hz, 2H, H-2'/6'), 7.21 (bd.s, 1H, H-6''), 7.47 (d, $J = 8.8$ Hz, 2H, H-2/6), 8.68 (s, 1H, =CH); EI-MS m/z (% rel. abund.): 460 (M^+ , 100), 126 (32), 252 (24), 266 (92), 314 (28), 417 (29), 417 (29); Anal. calcd. for $\text{C}_{27}\text{H}_{32}\text{N}_4\text{O}_3$: (460.56): N, 12.16; H, 7.00; C, 70.41; Found: N, 12.15; H, 7.01; C, 70.40.

3.9. 3-[[bis-(4-dimethylamino-phenyl)-methylene]-hydrazone-methyl]-phenol (7)

Yield: 0.232 g (79 %); $^1\text{H NMR}$ (400 MHz, $\text{DMSO-}d_6$): δ 2.96 (s, 12H, $-\text{NCH}_3$), 6.68 (d, $J = 8.8$ Hz, 2H, H-3/5), 6.80 (d, $J = 8.0$ Hz, 2H, H-3'/5'), 6.90 (m, 1H, H-2''), 7.12 (t, $J = 8.4$ Hz, 1H, H-5''), 7.22 (d, $J = 8.0$ Hz, 1H, H-4''), 7.28 (d, $J = 8.4$ Hz, 1H, H-6''), 7.28 (d, $J = 8.8$ Hz, 2H, H-2'/6'), 7.44 (d, $J = 8.8$ Hz, 2H, H-2/6), 8.69 (s, 1H, =CH), 11.68 (br.s, 1H, $-\text{OH}$); EI-MS m/z (% rel. abund.): 401 (M^+ , 100), 126 (35), 226 (20), 266 (83), 293 (13), 386 (5); Anal. calcd. for $\text{C}_{25}\text{H}_{29}\text{N}_4\text{O}$ (401.52): N, 13.95; H, 7.28; C, 74.78; Found: N, 13.94; H, 7.29; C, 74.77.

3.10. 2-*[bis-(4-dimethylamino-phenyl)-methylene]-hydrazonomethyl*]-4-nitro-phenol (8)

Yield: 0.260 g (83 %); $^1\text{H NMR}$ (400 MHz, DMSO- d_6): δ 2.96 (s, 12H, $-\text{NCH}_3$), 6.73 (d, $J = 2\text{ Hz}$, H-3/5), 6.78 (d, $J = 8.8\text{ Hz}$, 2H, H-3'/5'), 7.00 (d, $J = 8.8\text{ Hz}$, 1H, H-3''), 7.11 (d, $J = 8.8\text{ Hz}$, 2H, H-2'/6'), 7.51 (d, $J = 8.8\text{ Hz}$, 2H, H-2/6), 8.14 (dd, $J = 11.6\text{ Hz}$, 1H, H-4''), 8.55 (d, $J = 2.8\text{ Hz}$, 1H, H-6''), 8.69 (s, 1H, $=\text{CH}$), 11.68 (br.s, 1H, $-\text{OH}$); EI-MS m/z (% rel. abund.): 430 (M^+ , 100), 126 (36), 145 (10), 223 (12), 250 (14), 266 (85), 267 (22); Anal. calcd. for $\text{C}_{24}\text{H}_{25}\text{N}_5\text{O}_3$ (430.48): N, 16.23; H, 5.84; C, 66.81; Found: N, 16.22; H, 5.85; C, 66.80.

3.11. 2-*[bis-(4-dimethylamino-phenyl)-methylene]-hydrazonomethyl*]-6-methoxy-phenol (9)

Yield: 0.251 g (82 %); $^1\text{H NMR}$ (400 MHz, DMSO- d_6): δ 2.96 (s, 12H, $-\text{NCH}_3$), 3.72 (s, 3H, $-\text{OCH}_3$), 6.72 (d, $J = 8.8\text{ Hz}$, 1H, H-4''), 6.76 (d, $J = 8.8\text{ Hz}$, 2H, H-3/5), 6.78 (d, $J = 8.8\text{ Hz}$, 2H, H-3'/5'), 6.83 (t, $J = 8.0\text{ Hz}$, 1H, H-5''), 7.00 (d, $J = 8.0\text{ Hz}$, 1H, H-6''), 7.49 (d, $J = 8.8\text{ Hz}$, 2H, H-2'/6'), 7.58 (d, $J = 8.8\text{ Hz}$, 2H, H-2/6), 8.69 (s, 1H, $=\text{CH}$), 11.68 (br.s, 1H, $-\text{OH}$); EI-MS m/z (% rel. abund.): 416 (M^+ , 100), 105 (9), 126 (61), 146 (15), 223 (31), 266 (98), 293 (16), 399 (24); Anal. calcd. for $\text{C}_{25}\text{H}_{28}\text{N}_4\text{O}_2$ (416.51): N, 13.45; H, 6.78; C, 72.09; Found: N, 13.46; H, 6.79; C, 72.08.

3.12. Bis-(4-dimethylamino-phenyl)-methylene-hydrazonomethyl-2,4-diimethoxy-benzene (10)

Yield: 0.234 g (79 %); $^1\text{H NMR}$ (400 MHz, DMSO- d_6): δ 2.96 (s, 12H, $-\text{NCH}_3$), 3.78 (s, 3H, $-\text{OCH}_3$), 6.73 (d, $J = 4.0\text{ Hz}$, 4H, H-3/5, H-3'/5'), 7.00 (d, $J = 8.0\text{ Hz}$, 1H, H-3''), 7.16 (d, $J = 8.8\text{ Hz}$, 2H, H-2'/6'), 7.22 (d, $J = 8.8\text{ Hz}$, 1H, H-5''), 7.27 (d, $J = 1.2\text{ Hz}$, 1H, H-6''), 7.46 (d, $J = 8.8\text{ Hz}$, 2H, H-2/6), 8.69 (s, 1H, $=\text{CH}$); EI-MS m/z (% rel. abund.): 430 (M^+ , 100), 126 (14), 223 (22), 266 (75), 412 (17); Anal. calcd. for $\text{C}_{26}\text{H}_{30}\text{N}_4\text{O}_2$ (430.54): N, 13.01; H, 7.02; C, 72.53; Found: N, 13.02; H, 7.03; C, 72.52.

3.13. Bis-(4-dimethylamino-phenyl)-methylene-hydrazonomethyl-3-methyl-benzene (11)

Yield: 0.232 g (79 %); $^1\text{H NMR}$ (400 MHz, DMSO- d_6): δ 2.35 (s, 3H, $-\text{CH}_3$), 2.96 (s, 12H, $-\text{NCH}_3$), 6.71 (d, $J = 8.0\text{ Hz}$, 4H, H-3/5, H-3'/5'), 7.12 (d, $J = 8.8\text{ Hz}$, 2H, H-3''/5''), 7.22 (d, $J = 7.6\text{ Hz}$, 2H, H-2''/6''), 7.45 (d, $J = 8.0\text{ Hz}$, 2H, H-2'/6'), 7.55 (d, $J = 8.0\text{ Hz}$, 2H, H-2/6), 8.69 (s, 1H, $=\text{CH}$); EI-MS m/z (% rel. abund.): 384 (M^+ , 100), 77 (12), 105 (13), 126 (35), 148 (66), 224 (50), 251 (27), 266 (78), 293 (16), 356 (19); Anal. calcd. for $\text{C}_{25}\text{H}_{28}\text{N}_4$ (384.51): 14.57; H, 7.34; N, C, 78.09; Found: N, 14.55; H, 7.35; C, 78.11.

3.14. Bis-(4-dimethylamino-phenyl)-methylene-hydrazonomethyl-4-nitro-benzene (12)

Yield: 0.240 g (80 %); $^1\text{H NMR}$ (400 MHz, DMSO- d_6): δ 2.96 (s, 12H, $-\text{NCH}_3$), 6.71 (d, $J = 8.8\text{ Hz}$, 4H, H-3/5, H-3'/5'), 7.12 (d, $J = 8.4\text{ Hz}$, 2H, H-2'/6'), 7.48 (d, $J = 8.8\text{ Hz}$, 2H, H-2/6), 7.90 (d, $J = 8.8\text{ Hz}$, 2H, H-2''/6''), 8.27 (d, $J = 8.8\text{ Hz}$, 2H, H-3''/5''), 8.69 (s, 1H, $=\text{CH}$); EI-MS m/z (% rel. abund.): 415 (M^+ , 100), 105 (7), 126 (26), 252 (18), 266 (72), 385 (21); Anal. calcd. for $\text{C}_{24}\text{H}_{25}\text{N}_5\text{O}_2$ (415.48): N, 16.86; H, 6.06; C, 69.38; Found: N, 16.85; H, 6.08; C, 69.39.

3.15. Bis-(4-dimethylamino-phenyl)-methylene-hydrazonomethyl-2-chloro-benzene (13)

Yield: 0.201 g (72 %); $^1\text{H NMR}$ (400 MHz, DMSO- d_6): δ 2.96 (s, 12H, $-\text{NCH}_3$), 6.69 (d, $J = 8.8\text{ Hz}$, 4H, H-3/5, H-3'/5'), 6.74 (t, $J = 8.8\text{ Hz}$, 2H, H-4''/5''), 7.15 (d, $J = 8.4\text{ Hz}$, 2H, H-3''/6''), 7.43 (d, $J = 8.8\text{ Hz}$, 2H, H-2/6), 7.58 (d, $J = 8.4\text{ Hz}$, 2H, H-2'/6'), 7.89 (d, $J = 8.0\text{ Hz}$, 2H, H-2/6), 8.69 (s, 1H, $=\text{CH}$); EI-MS m/z (% rel. abund.): 404 (M^+ , 100), 126 (17), 223 (17), 252 (17), 266 (74), 376 (10); Anal. calcd. for $\text{C}_{24}\text{H}_{25}\text{ClN}_4$ (404.93): N, 13.84; H, 6.22; C, 71.19; Found: N, 13.85; H, 6.21; C, 71.20.

3.16. Bis-(4-dimethylamino-phenyl)-methylene-hydrazonomethyl-4-dimethylamino-benzene (14)

Yield: 0.242 g (87 %); $^1\text{H NMR}$ (400 MHz, DMSO- d_6): δ 2.96 (s, 18H, $-\text{NCH}_3$), 6.66 (d, $J = 8.0\text{ Hz}$, 2H, H-3''/5''), 6.69 (d, $J = 8.8\text{ Hz}$, 4H, H-3/5, H-3'/5'), 7.43 (d, $J = 8.8\text{ Hz}$, 2H, H-2'/6'), 7.55 (d, $J = 8.8\text{ Hz}$, 2H, H-2''/6''), 7.60 (d, $J = 8.8\text{ Hz}$, 2H, H-2/6), 8.69 (s, 1H, $=\text{CH}$); EI-MS m/z (% rel. abund.): 413 (M^+ , 100), 145 (10), 223 (13), 252 (14), 266 (43), 293 (23), 385 (27); Anal. calcd. for $\text{C}_{26}\text{H}_{31}\text{N}_5$ (413.55): N, 16.93; H, 7.56; C, 75.51; Found: N, 16.92; H, 7.55; C, 75.50.

3.17. 3-*[bis-(4-dimethylamino-phenyl)-methylene]-hydrazonomethyl*]-benzaldehyde (15)

Yield: 0.251 g (86 %); $^1\text{H NMR}$ (400 MHz, DMSO- d_6): δ 2.96 (s, 12H, $-\text{NCH}_3$), 6.73 (d, $J = 8.8\text{ Hz}$, 4H, H-3/5, H-3'/5'), 7.47 (d, $J = 8.8\text{ Hz}$, 2H, H-2'/6'), 7.57 (d, $J = 8.8\text{ Hz}$, 2H, H-2/6), 7.70 (s, 1H, H-2''), 7.86 (d, $J = 8.0\text{ Hz}$, 1H, H-6''), 7.86 (d, $J = 8.0\text{ Hz}$, 1H, H-6'), 7.86 (d, $J = 8.0\text{ Hz}$, 1H, H-6), 7.94 (d, $J = 8.0\text{ Hz}$, 1H, H-4''), 8.10 (t, $J = 8.0\text{ Hz}$, 1H, H-5''), 8.69 (s, 2H, $=\text{CH}$); EI-MS m/z (% rel. abund.): 398 (M^+ , 100), 77 (10), 120 (12), 126 (26), 148 (65), 159 (14), 224 (25), 268 (49); Anal. calcd. for $\text{C}_{25}\text{H}_{26}\text{N}_4\text{O}$ (398.50): N, 14.06; H, 6.58; C, 75.35; Found: N, 14.05; H, 6.59; C, 75.36.

3.18. Bis-(4-dimethylamino-phenyl)-methylene-hydrazonomethyl-naphthalen (16)

Yield: 0.270 g (89 %); $^1\text{H NMR}$ (400 MHz, DMSO- d_6): δ 2.96 (s, 12H, -NCH $_3$), 7.05 (d, J = 8.0 Hz, 1H, H-2''), 7.16 (d, J = 8.0 Hz, 5H, H-3/5, H-3'/5', H-5''), 7.27 (s, 1H, H-3''), 7.47 (d, J = 8.8 Hz, 4H, H-2/6, 2'/6'), 8.44 (s, 1H, H-10''), 8.69 (s, 2H, =CH); EI-MS m/z (% rel. abund.): 420 (M^+ , 100), 77 (6), 126 (16), 223 (19), 266 (70), 284 (18), 387 (12); Anal. calcd. for C $_{28}$ H $_{28}$ N $_4$ (420.54): N, 13.32; H, 6.71; C, 79.97; Found: N, 13.31; H, 6.72; C, 79.96.

3.19. 4-[[bis-(4-dimethylamino-phenyl)-methylene]-hydrazonomethyl]-benzene-1,2-diol (17)

Yield: 0.262 g (85 %); $^1\text{H NMR}$ (400 MHz, DMSO- d_6): δ 2.96 (s, 12H, -NCH $_3$), 6.71 (d, J = 8.8 Hz, 5H, H-3/5, H-3'/5', H-5''), 7.11 (d, J = 8.8 Hz, 1H, H-6''), 7.47 (d, J = 8.0 Hz, 2H, H-2'/6'), 7.67 (d, J = 8.4 Hz, 2H, H-2/6, H-2''), 8.69 (s, 1H, =CH), 11.68 (br.s, 2H, -OH); EI-MS m/z (% rel. abund.): 402 (M^+ , 100), 126 (21), 223 (22), 250 (13), 266 (68), 385 (21); Anal. calcd. for C $_{24}$ H $_{26}$ N $_4$ O $_2$ (402.48): N, 13.92; H, 6.51; C, 71.62; Found: N, 13.93; H, 6.50; C, 71.61.

3.20. Bis-(4-dimethylamino-phenyl)-methylene-hydrazonomethyl-4-chloro-benzene (18)

Yield: 0.300 g (90 %); $^1\text{H NMR}$ (400 MHz, DMSO- d_6): δ 2.96 (s, 12H, -NCH $_3$), 6.69 (d, J = 8.8 Hz, 4H, H-3/5, H-3'/5'), 7.11 (t, J = 9.2 Hz, 2H, H-3'/5''), 7.29 (d, J = 8.8 Hz, 2H, H-2'/6'), 7.42 (d, J = 8.4 Hz, 4H, H-2/6, H-2''/6''), 8.69 (s, 1H, =CH); EI-MS m/z (% rel. abund.): 404 (M^+ , 100), 119 (5), 126 (16), 223 (17), 252 (17), 266 (74), 376 (10); Anal. calcd. for C $_{24}$ H $_{25}$ ClN $_4$ (404.93): N, 13.84; H, 6.22; C, 71.19; Found: N, 13.82; H, 6.23; C, 71.18.

3.21. Bis-(4-dimethylamino-phenyl)-methylene-hydrazonomethyl-3,4-dimethoxy-benzene (19)

Yield: 0.230 g (82 %); $^1\text{H NMR}$ (400 MHz, DMSO- d_6): δ 2.96 (s, 12H, -NCH $_3$), 3.78 (s, 6H, -OCH $_3$), 6.72 (d, J = 8.8 Hz, 5H, H-3/5 H-3'/5', H-5''), 7.00 (d, J = 8.0 Hz, 1H, H-6''), 7.16 (d, J = 8.4 Hz, 2H, H-2'/6'), 7.27 (s, 1H, H-2''), 7.46 (d, J = 8.8 Hz, 2H, H-2/6), 8.69 (s, 1H, =CH); EI-MS m/z (% rel. abund.): 430 (M^+ , 100), 77 (6), 126 (25), 223 (14), 252 (17), 266 (69), 387 (13); Anal. calcd. for C $_{26}$ H $_{30}$ N $_4$ O $_2$ (430.54): N, 13.01; H, 7.02; C, 72.53; Found: N, 13.00; H, 7.03; C, 72.52.

3.22. 4-[[bis-(4-dimethylamino-phenyl)-methylene]-hydrazonomethyl]-benzene-1,2,3-triol (20)

Yield: 0.281 g (84 %); $^1\text{H NMR}$ (400 MHz, DMSO- d_6): δ 2.96 (s, 12H, -NCH $_3$), 6.36 (d, J = 8.4 Hz, 1H, H-5''), 6.70 (d, J = 8.8 Hz, 1H, H-6''), 6.77 (d, J = 8.8 Hz, 2H, H-3/5), 6.81 (d, J = 8.4 Hz, 2H, H-3'/5'), 7.10 (d, J = 8.4 Hz, 2H, H-2'/6'), 7.45 (d, J = 8.8 Hz, 2H, H-2/6), 8.69 (s, 1H, =CH), 11.68 (br.s, 3H, -OH); EI-MS m/z (% rel. abund.): 418 (M^+ , 100), 120 (8), 126 (16), 146 (10), 153 (9), 223 (31), 250 (17), 266 (66); Anal. calcd. for C $_{24}$ H $_{26}$ N $_4$ O $_3$ (418.48): N, 13.39; H, 6.26; C, 68.88; Found: N, 13.38; H, 6.27; C, 68.87.

3.23. 2-[[bis-(4-dimethylamino-phenyl)-methylene]-hydrazonomethyl]-4-bromo-phenol (21)

Yield: 0.221 g (78 %); $^1\text{H NMR}$ (400 MHz, DMSO- d_6): δ 2.96 (s, 12H, -NCH $_3$), 6.45 (d, J = 9.2 Hz, 1H, H-3''), 6.76 (d, J = 8.4 Hz, 4H, H-3/5, H-3'/5'), 7.09 (d, J = 8.8 Hz, 2H, H-2'/6'), 7.40 (dd, J = 8.8 Hz, 1H, H-4''), 7.49 (d, J = 8.8 Hz, 2H, H-2/6), 7.72 (d, J = 2.4 Hz, 1H, H-6''), 8.69 (s, 1H, =CH), 11.68 (br.s, 3H, -OH); EI-MS m/z (% rel. abund.): 465 (M^+ , 100), 126 (32), 145 (6), 226 (18), 252 (14), 266 (89), 293 (14), 396 (66); Anal. calcd. for C $_{24}$ H $_{25}$ BrN $_4$ O (465.38): N, 12.04; H, 5.41; C, 61.94; Found: N, 12.05; H, 5.40; C, 61.93.

3.24. Bis-(4-dimethylamino-phenyl)-methylene-hydrazonomethyl-4-methylsulfanyl-benzene (22)

Yield: 0.232 g (80 %); $^1\text{H NMR}$ (400 MHz, DMSO- d_6): δ 2.86 (s, 12H, -NCH $_3$), 3.78 (s, 3H, -SCH $_3$), 6.71 (d, J = 8.8 Hz, 4H, H-3/5 H-3'/5'), 7.12 (d, J = 8.8 Hz, 2H, H-3'/5''), 7.28 (d, J = 8.0 Hz, 2H, H-2'/6'), 7.45 (d, J = 8.8 Hz, 2H, H-2'/6'), 7.59 (d, J = 8.4 Hz, 2H, H-2/6), 8.69 (s, 1H, =CH); EI-MS m/z (% rel. abund.): 416 (M^+ , 100), 77 (5), 105 (5), 126 (52), 223 (13), 252 (19), 266 (83), 293 (15), 388 (14); Anal. calcd. for C $_{25}$ H $_{28}$ N $_4$ S (416.58): N, 13.45; H, 6.77; C, 72.08; Found: N, 13.44; H, 6.78; C, 72.09.

3.25. Bis-(4-dimethylamino-phenyl)-methylene]-hydrazonomethyl]-2-methyl-benzene (23)

Yield: 0.203 g (82 %); $^1\text{H NMR}$ (400 MHz, DMSO- d_6): δ 2.49 (s, 3H, -CH $_3$), 2.96 (s, 12H, -NCH $_3$), 6.71 (d, J = 8.4 Hz, 4H, H-3/5, H-3'/5'), 7.13 (d, J = 8.8 Hz, 2H, H-2'/6'), 7.21 (t, J = 6.4 Hz, 1H, H-4''), 7.29 (m, 2H, H-3'/5'), 7.47 (d, J = 8.8 Hz, 2H, H-2/6), 7.66 (d, J = 7.2 Hz, 1H, H-6''), 8.69 (s, 1H, =CH); EI-MS m/z (% rel. abund.): 384 (M^+ , 100), 91 (6), 105 (8), 126 (52), 148 (9), 223 (39), 237 (11), 251 (70), 266 (88), 369 (22); Anal. calcd. for C $_{25}$ H $_{28}$ N $_4$ (384.51): N, 14.57; H, 7.34; C, 78.09; Found: N, 14.56; H, 7.35; C, 78.08.

3.26. Bis-(4-dimethylamino-phenyl)-methylene]-hydrazonomethyl]-4-methoxy-benzene (24)

Yield: 0.250 g (85 %); $^1\text{H NMR}$ (400 MHz, DMSO- d_6): δ 2.96 (s, 12H, -NCH $_3$), 3.73 (s, 3H, -OCH $_3$), 6.72 (d, J = 8.8 Hz, 4H, H-3/5, H-3'/5'), 6.98 (d, J = 8.8 Hz, 1H, H-3''), 7.04 (d, J = 8.8 Hz, 1H, H-5''), 7.13 (d, J = 8.8 Hz, 1H, H-2''), 7.44 (d, J = 8.8 Hz, 2H, H-2'/6'),

8.697.59 (d, $J = 8.8$ Hz, 2H, H-2/6), 7.80 (d, $J = 8.8$ Hz, 1H, H-6''), (s, 1H, =CH); EI-MS m/z (% rel. abund.): 400 (M^+ , 100), 77 (6), 126 (18), 223 (7), 254 (11), 266 (52), 293 (11), 372 (13); Anal. calcd. for $C_{25}H_{28}N_4O$ (400.51): N, 13.99; H, 7.05; C, 74.97; Found: N, 13.97; H, 7.03; C, 74.96.

3.27. Bis-(4-dimethylamino-phenyl)-methylene-hydrazonomethyl-3-nitro-benzene (25)

Yield: 0.242 g (87 %); 1H NMR (400 MHz, DMSO- d_6): δ 2.96 (s, 12H, $-NCH_3$), 6.68 (d, $J = 8.8$ Hz, 4H, H-3/5, H-3'/5'), 7.15 (d, $J = 8.4$ Hz, 2H, H-2'/6), 7.28 (d, $J = 8.4$ Hz, 2H, H-2/6), 7.71 (t, $J = 8.4$ Hz, 1H, H-5''), 8.32 (d, $J = 7.6$ Hz, 1H, H-6''), 8.37 (t, $J = 8.0$ Hz, 1H, H-4''), 8.69 (s, 1H, =CH), 8.70 (d, $J = 10$ Hz, 1H, H-2''); EI-MS m/z (% rel. abund.): 415 (M^+ , 100), 77 (6), 118 (13), 126 (45), 145 (8), 208 (8), 237 (13), 252 (26), 266 (97), 293 (11), 385 (17); Anal. calcd. for $C_{24}H_{25}N_5O_2$ (415.48): N, 16.86; H, 6.06; C, 69.38; Found: N, 16.87; H, 6.05; C, 69.39.

3.28. 4-[[bis-(4-dimethylamino-phenyl)-methylene]-hydrazonomethyl]-phenol (26)

Yield: 0.233 g (82 %); 1H NMR (400 MHz, DMSO- d_6): δ 2.96 (s, 12H, $-NCH_3$), 6.71 (d, $J = 8.8$ Hz, 4H, H-3/5, H-3'/5'), 7.10 (d, $J = 8.4$ Hz, 4H, H-2'/6, H-2'/6'), 7.11 (d, $J = 8.8$ Hz, 2H, H-3'/5'), 7.28 (d, $J = 6.8$ Hz, 2H, H-2'/6'), 8.69 (s, 1H, =CH), 11.68 (br.s, 1H, -OH); EI-MS m/z (% rel. abund.): 386 (M^+ , 100), 77 (6), 105 (8), 126 (32), 226 (18), 237 (10), 252 (22), 266 (89), 293 (14), 358 (13); Anal. calcd. for $C_{24}H_{26}N_4O$ (386.489): N, 14.50; H, 6.78; C, 74.58; Found: N, 14.51; H, 6.79; C, 74.57.

3.29. 3-[[bis-(4-dimethylamino-phenyl)-methylene]-hydrazonomethyl]-naphthalen-2-ol (27)

Yield: 0.282 g (84 %); 1H NMR (400 MHz, DMSO- d_6): δ 2.69 (s, 12H, $-NCH_3$), 6.74 (d, $J = 8.8$ Hz, 2H, H-3/5), 6.80 (d, $J = 8.8$ Hz, 2H, H-3'/5'), 7.07 (d, $J = 8.8$ Hz, 1H, H-3'), 7.15 (d, $J = 8.8$ Hz, 4H, H-2/6, H-2'/6'), 7.37 (t, $J = 7.2$ Hz, 1H, H-5''), 7.54 (t, $J = 8.8$ Hz, 1H, H-8''), 7.86 (m, 2H, H-6'/7'), 8.38 (d, $J = 8.4$ Hz, 1H, H-10''), 8.69 (s, 1H, =CH), 11.68 (br.s, 1H, -OH); EI-MS m/z (% rel. abund.): 436 (M^+ , 100), 77 (6), 105 (8), 126 (37), 170 (10), 223 (40), 250 (19), 266 (78), 419 (97); Anal. calcd. for $C_{28}H_{28}N_4O$ (436.54): N, 12.83; H, 6.46; C, 77.04; Found: N, 12.83; H, 6.46; C, 77.04.

3.30. α -Glucosidase inhibitory assay

The assessment of α -glucosidase inhibition activity was conducted with slight modifications, following the procedure outlined by Ref. [34]. In a total volume of 100 μ L of the reaction mixture, 70 μ L of 50 mM phosphate buffer at pH 6.8 was combined with 10 μ L of the investigated compound (0.5 mM in methanol per well), then added 10 μ L of enzyme solution (0.057 units, Sigma Inc.) in buffer solution. These mixed solutions were pre-incubated for 10 min after mixing at 37 $^\circ$ C, and pre-read. After this, the reaction was initiated by adding 10 μ L of 0.5 mM substrates (*p*-nitrophenyl α -D-glucopyranoside, Sigma Inc.). After 30-min incubation at 37 $^\circ$ C, the absorbance of *p*-nitro phenol was measured at 400 nm using the Synergy HT 96-well plate reader from BioTek, USA. Acarbose served as the standard reference. All these experiments were conducted in triplicate.

The kinetic experiments were performed by following a similar procedure as the method used for screening and IC_{50} calculation. To assess the mechanism of action of the selected compounds we used four different concentrations of the substrate (*p*-nitrophenyl α -D-glucopyranoside) including, 0.1, 0.2, 0.4 and 0.8 mM. In this study we used Lineweaver-Burk plots that determine the type of inhibition of the given compounds **8** and **9**, in which reciprocal of the reaction rate was plotted vs the reciprocal of substrate concentrations to investigate their effect on the K_m and V_{max} of the α -glucosidase. In such type of inhibition, V_{max} of the enzyme remains constant while K_m increases which is clearly showed by the Lineweaver-Burk plots (Figures: 8-unit A). Furthermore, we also identified the dissociation constant value the K_i values for compounds **8** and **9** evaluated for kinetics study. The secondary replot of Lineweaver-Burk plots were applied by taking slope of each line in Lineweaver-Burk plots vs different concentrations of compounds **8** and **9**. Further Dixon plots were used by plotting reciprocal of the rate of reaction of α -glucosidase vs different concentrations of the tested compounds (Fig. 8).

3.31. Statistical analysis

The programs were employed to analyze the attained results for biological activity, the SoftMax Pro package and Excel were utilized.

The given formula below was used to calculate percent inhibition.

$$\%Inhibition = 100 - \left(\frac{O.D_{test\ compound}}{O.D_{control}} \right) \times 100 \quad (1)$$

EZ-FIT (Perrella Scientific, Inc., USA) was used for IC_{50} calculations of all tested samples. To overcome on the expected errors all experiments were performed in triplicate, and variations in the results are reported in Standard Error of Mean values (SEM).

$$SE = \frac{\sigma}{\sqrt{n}} \quad (2)$$

3.32. Protocol of cytotoxicity (MTT) assay

Cytotoxicity of bis-benzimidazole derivatives was determined by the method reported by Pauwels. et al., [35]. In this experiment, all the compounds were evaluated at 30 μM in triplicate. Those compounds which showed >50 % inhibition at 30 μM , their IC_{50} value was determined at different concentration of the compounds from 30 to 0.9375 μM , however, compounds with <50 % inhibition at 30 μM were declared as inactive.

3.33. Molecular docking

To understand how the synthesized compounds interact with the binding pocket of the α -glucosidase enzyme, we employed the Molecular Operating Environment (MOE) software to dock these compounds. The docking process followed the protocol outlined in homology modeling [36], The forecasted 3D structure of *Saccharomyces cerevisiae*'s α -glucosidase involved predicting the primary sequence, obtained from UniProt (Access code P53341). A template search, conducted using Protein BLAST against the Protein Data Bank (PDB), identified the crystallographic structure of *Saccharomyces cerevisiae* isomaltase (PDB code 3AJ7; Resolution 1.30 Å). This template, chosen for its highest sequence identity of 72.4 % with the target, served as the basis for predicting the α -glucosidase structure. Ten distinct models of α -glucosidase were generated and refined using the AMBER99 forcefield, with the optimal model selected and subjected to evaluation. The generated model underwent energy minimization until reaching 0.05 gradients. Assessment of the modeled structure's quality was performed through Ramachandran and ProSA plots. The evaluation of backbone Psi and Phi dihedral angles for the α -glucosidase model indicated that 94.8 % of residues resided in the favored region, 4.8 % in the allowed region, and a mere 0.3 % in the outlier region. ProSA analysis revealed a Z-value of -10.70 , signifying no significant deviation from the score determined for proteins of similar size. Both Ramachandran and ProSA plots' outcomes underscore the accuracy of our modeled structure, affirming its suitability for implementation in the docking protocol.

The Molecular Builder Module program within MOE was employed to construct the 3D structures for all the synthesized compounds, and these structures were subsequently saved as (mdb) files for molecular docking. Following this, the energy of each constructed structure was minimized up to 0.05 Gradient using the MMFF94s force field implemented in MOE.

The active site of the protein served as the docking location for all compounds, utilizing the Triangular Matching docking method with default settings. Each compound underwent the generation of 10 different conformations during the docking process, allowing flexibility for ligands to achieve minimum energy structures. The software ranked the ligands based on scores obtained from GBVI/WSA binding free energy calculations in the S field, representing the score at the final stage. GBVI/WSA is a scoring function that estimates the binding free energy of the ligand in a given pose. In all scoring functions, lower scores indicate more favorable poses, and the unit for these scoring functions is kcal/mol. The top ranked conformation for each compound was chosen based on the docking score (S) for subsequent analysis. Following the docking process, the anticipated ligand-protein complexes were scrutinized for molecular interactions, and their 3D images were generated using LigPlot, a tool implemented in MOE.

3.34. MD simulation

Amber 22 software was used to run MD simulations for the most potent compounds in complex with the receptor [23]. The receptor and ligand's topology were generated using the tleap program. The FF14SB was employed as the protein force field while GAFF2 was used as the ligand force field. A cubic box with a size of 8 Å was employed for the systems' solvation [24]. For system neutralization, Na⁺ or Cl⁻ counter ions were supplied [25]. To reduce the energy of the systems, the two algorithms steepest descent and conjugate gradients were applied. The NVT ensemble was utilized for system equilibration at a constant pressure of 1 bar and temperature of 300 K. The SHAKE method was used to constrain the H-atoms. Finally, 30 ns of production runs were completed for each complex. The analysis of the MD simulation was performed using the CPPTRAJ module. For graphical representation Origin ProLab 2021 was used [26].

4. Conclusions

In the present study twenty seven Schiff base derivatives of benzophenone were synthesized, characterized and evaluated for α -glucosidase inhibitory activity. Except five compounds **11**, **20**, **21**, **25** and **27**, all other synthetic compounds showed good to moderate inhibitory activity. Four compounds **12**, **8**, **9**, and **5** exhibited comparable activity with the standard acarbose and were the most active compounds of the library having IC_{50} values of 0.28 ± 3.13 , 0.28 ± 2.65 , 0.29 ± 0.93 , 0.29 ± 4.67 μM , respectively. Kinetic studies of compounds **8** and **9** were also carried out which demonstrated a concentration dependent pattern of inhibition. The *in-silico* studies of the synthetic compounds also supported the *in vitro* data and showed that these compounds bound well within the enzyme pocket. The synthetic compounds **1–27** can serve as lead molecules for the treatment of diabetes, further studies on these compounds might help in development of new drugs.

Funding

The authors extend their appreciation to the Deanship of Scientific Research at King Khalid University for funding this work through the Large Groups Project under grant number (RGP. 2/100/44)

Availability of data and materials

All datasets on which the conclusions of the manuscript rely are presented in the paper.

Consent for publication

Not applicable.

Ethics approval

Not applicable.

CRedit authorship contribution statement

Momin Khan: Methodology, Conceptualization. **Ghulam Ahad:** Methodology, Data curation. **Aftab Alam:** Writing – original draft, Methodology. **Saeed Ullah:** Methodology, Formal analysis. **Ajmal Khan:** Writing – review & editing, Conceptualization. **Kanwal:** Investigation, Data curation. **Uzma Salar:** Investigation, Data curation. **Abdul Wadood:** Visualization, Software, Methodology. **Amar Ajmal:** Visualization, Software. **Khalid Mohammed Khan:** Supervision, Data curation, Conceptualization. **Shahnaz Perveen:** Writing – review & editing, Formal analysis. **Jalal Uddin:** Validation, Software, Investigation. **Ahmed Al-Harrasi:** Writing – review & editing, Supervision, Funding acquisition.

Declaration of competing interest

The authors declare that they have no known competing financial interests or personal relationships that could have appeared to influence the work reported in this paper.

Acknowledgments

The authors extend their appreciation to the Deanship of Scientific Research at King Khalid University for funding this work through the Large Groups Project under grant number (RGP. 2/100/44)

Appendix A. Supplementary data

Supplementary data to this article can be found online at <https://doi.org/10.1016/j.heliyon.2023.e23323>.

References

- [1] R. Xu, et al., Bimetallic AuRu aerogel with enzyme-like activity for colorimetric detection of Fe²⁺ and glucose, *Chin. Chem. Lett.* 33 (10) (2022) 4683–4686.
- [2] X.-F. He, et al., Tsaokols A and B, unusual flavanol-monoterpenoid hybrids as α -glucosidase inhibitors from *Amomum tsao-ko*, *Chin. Chem. Lett.* 32 (3) (2021) 1202–1205.
- [3] E.B. de Melo, A. da Silveira Gomes, I. Carvalho, α - and β -Glucosidase inhibitors: chemical structure and biological activity, *Tetrahedron* 62 (44) (2006) 10277–10302.
- [4] N. Asano, Glycosidase inhibitors: update and perspectives on practical use, *Glycobiology* 13 (10) (2003) 93R–104R.
- [5] Y. Li, et al., Phenoxazine-based supramolecular tetrahedron as biomimetic lectin for glucosamine recognition, *Chin. Chem. Lett.* 32 (2) (2021) 735–739.
- [6] Z. Gao, et al., Automatic interpretation and clinical evaluation for fundus fluorescein angiography images of diabetic retinopathy patients by deep learning, *Br. J. Ophthalmol.* 107 (12) (2022) 1852–1858.
- [7] T. Arshad, et al., Syntheses, in vitro evaluation and molecular docking studies of 5-bromo-2-aryl benzimidazoles as α -glucosidase inhibitors, *Med. Chem. Res.* 25 (9) (2016) 2058–2069.
- [8] U. Salar, et al., Syntheses of new 3-thiazolyl coumarin derivatives, in vitro α -glucosidase inhibitory activity, and molecular modeling studies, *Eur. J. Med. Chem.* 122 (2016) 196–204.
- [9] F. Ali, et al., Hydrazinyl arylthiazole based pyridine scaffolds: synthesis, structural characterization, in vitro α -glucosidase inhibitory activity, and in silico studies, *Eur. J. Med. Chem.* 138 (2017) 255–272.
- [10] M.U. Ahmad, et al., Syntheses of benzimidazole based hydrazones as non-sugar based α -glucosidase inhibitors: structure activity relation and molecular docking, *Drug Dev. Res.* 82 (7) (2021) 1033–1043.
- [11] I. Khan, et al., Utilization of the common functional groups in bioactive molecules: exploring dual inhibitory potential and computational analysis of keto esters against α -glucosidase and carbonic anhydrase-II enzymes, *Int. J. Biol. Macromol.* 167 (2021) 233–244.
- [12] G. Cui, et al., Synthesis and characterization of Eu (III) complexes of modified D-glucosamine and poly (N-isopropylacrylamide), *Mater. Sci. Eng. C* 78 (2017) 603–608.
- [13] H.A. Al-ghulikhah, et al., Discovery of chalcone derivatives as potential α -glucosidase and cholinesterase inhibitors: effect of hyperglycemia in paving a path to dementia, *J. Mol. Struct.* 1275 (2023), 134658.
- [14] R.I. Alsantali, et al., Flavone-based hydrazones as new tyrosinase inhibitors: synthetic imines with emerging biological potential, SAR, molecular docking and drug-likeness studies, *J. Mol. Struct.* 1251 (2022), 131933.
- [15] E.U. Mughal, et al., Design and synthesis of 2-amino-4, 6-diarylpyrimidine derivatives as potent α -glucosidase and α -amylase inhibitors: structure–activity relationship, in vitro, QSAR, molecular docking, MD simulations and drug-likeness studies, *J. Biomol. Struct. Dyn.* (2023) 1–17.

- [16] Y. Shen, et al., Synthesis, characterization, and crystal structure of modified benzophenone UV-absorber containing reactive group, *Res. Chem. Intermed.* 42 (4) (2016) 2909–2918.
- [17] G. Dorman, G.D. Prestwich, Benzophenone photophores in biochemistry, *Biochemistry* 33 (19) (1994) 5661–5673.
- [18] S. Mahajan, et al., QSAR analysis of benzophenone derivatives as antimalarial agents, *Indian J. Pharmaceut. Sci.* 74 (1) (2012) 41.
- [19] O. Cuesta-Rubio, A.L. Piccinelli, L. Rastrelli, Chemistry and biological activity of polyisoprenylated benzophenone derivatives, *Stud. Nat. Prod. Chem.* 32 (2005) 671–720.
- [20] D.R. Scavenging, Synthesis of benzophenone hydrazone analogs and their DPPH radical scavenging and urease inhibitory activities, *J. Chem. Soc. Pakistan* 37 (3) (2015) 479.
- [21] K.M. Khan, et al., Anti-cancer potential of benzophenone-bis-schiff bases on human pancreatic cancer cell line, *J. Chem. Soc. Pakistan* 38 (5) (2016) 954–958.
- [22] G. Michael, J. Edith, C. Peter, Dietary antioxidant flavonoids and risk of coronary heart disease, *Lancet* 342 (1993) 1007–1011.
- [23] F.N. Khan, et al., 3-tert-Butyl-1H-isochromene-1-thione, *Acta Crystallogr., Sect. E: Struct. Rep. Online* 66 (6) (2010) o1470–o1470.
- [24] A. Arshia, et al., Synthesis and urease inhibitory activities of benzophenone semicarbazones/thiosemicarbazones, *Med. Chem. Res.* 25 (11) (2016) 2666–2679.
- [25] T. Beelders, et al., Benzophenone C- and O-glucosides from *Cyclopia genistoides* (honeybush) inhibit mammalian α -glucosidase, *J. Nat. Prod.* 77 (12) (2014) 2694–2699.
- [26] Q. Liu, et al., Synthesis and evaluation of benzophenone O-glycosides as α -glucosidase inhibitors, *Arch. Pharmazie* 345 (10) (2012) 771–783.
- [27] Arshia, et al., Anti-glycemic potential of benzophenone thio/semicarbazone derivatives: synthesis, enzyme inhibition and ligand docking studies, *J. Biomol. Struct. Dyn.* 40 (16) (2022) 7339–7350.
- [28] F. Begum, et al., Synthesis and urease inhibitory potential of benzophenone sulfonamide hybrid in vitro and in silico, *Bioorg. Med. Chem.* 27 (6) (2019) 1009–1022.
- [29] A. Arshia, et al., Synthesis and urease inhibitory activities of benzophenone semicarbazones/thiosemicarbazones, *Med. Chem. Res.* 25 (2016) 2666–2679.
- [30] A. Alam, et al., Novel Bis-Schiff's base derivatives of 4-nitroacetophenone as potent α -glucosidase agents: design, synthesis and in silico approach, *Bioorg. Chem.* 128 (2022), 106058.
- [31] K. Mohammed Khan, et al., Synthesis of benzophenonehydrazone Schiff bases and their in vitro antiglycating activities, *Med. Chem.* 9 (4) (2013) 588–595.
- [32] A.N. Aziz, et al., Synthesis, crystal structure, DFT studies and evaluation of the antioxidant activity of 3, 4-dimethoxybenzenamine Schiff bases, *Molecules* 19 (6) (2014) 8414–8433.
- [33] Danish Shahzad, et al., *Novel C-2 symmetric molecules as α -glucosidase and α -amylase inhibitors: design, synthesis, kinetic evaluation, molecular docking and pharmacokinetics*, *Molecules* 24 (8) (2019) 1511.
- [34] P. Chappelaine, R.R. Tremblay, J. Dube, P-Nitrophenol- α -D-glucopyranoside as substrate for measurement of maltase activity in human semen, *Clin. Chem.* 24 (2) (1978) 208–211.
- [35] R. Pauwels, et al., Rapid and automated tetrazolium-based colorimetric assay for the detection of anti-HIV compounds, *J. Virol Methods* 20 (4) (1988) 309–321.
- [36] L.R. Guerreiro, et al., Five-membered iminocyclitol α -glucosidase inhibitors: synthetic, biological screening and in silico studies, *Bioorg. Med. Chem.* 21 (7) (2013) 1911–1917.